

# POLITECNICO DI TORINO

Master's Degree in Biomedical Engineering

## **Prediction of the effects of Volatile Anesthetics on GABA<sub>A</sub> receptor in complex with GABA by Molecular Modelling**



**Politecnico  
di Torino**

### **Thesis Supervisor**

Prof. Marco Agostino Deriu

### **Candidate**

Alessandra Di Loreto

### **Co-supervisors**

Dr. Eric Adriano Zizzi

ACADEMIC YEAR 2024-2025



# Contents

<b>Abstract.....</b>	<b>6</b>
<b>1. Introduction .....</b>	<b>7</b>
<b>2. Biological Background .....</b>	<b>9</b>
2.1 An Introduction to Volatile Anesthetics (VAs).....	9
2.2 Mechanism of Action.....	10
2.3 Volatile Anesthetics .....	11
2.4 Ion Channels .....	13
2.4.1 Nicotinic Acetylcholine Receptor .....	14
2.4.2 Serotonin Type 3 Receptor.....	16
2.4.4 GABA and GABA <sub>A</sub> Receptor .....	17
<b>3. Materials and Methods .....</b>	<b>19</b>
3.1 Molecular Modeling .....	19
3.2 Molecular Mechanics .....	19
3.2.1 Potential Energy Function.....	20
3.2.2 Bonded Interactions.....	20
3.2.3 Non-Bonded Interactions .....	22
3.2.4 Periodic Boundary Conditions.....	24
3.2.5 Potential Energy Minimization .....	25
3.3 Molecular Dynamics.....	27
3.3.1 Statistical Ensemble.....	28
3.3.2 Molecular Dynamics Software .....	29
3.3.3 Principal Component Analysis.....	30
3.3.4 General Force Fields .....	31

<b>4. Interaction between <math>\alpha 1\beta 2\gamma 2</math> GABA A receptor and Volatile Anesthetics .....</b>	<b>33</b>
4.1 Introduction .....	33
4.2 Materials and Methods.....	34
4.2.1 Model building.....	37
4.2.2 Molecular Dynamics .....	39
4.2.3 Results .....	41
4.3 Discussion.....	51
4.4 Conclusion .....	53
<b>5. References .....</b>	<b>54</b>



# Abstract

Anesthesia, the reversible pharmacological suspension of conscious brain activity, is a cornerstone of modern surgery and has been one of the main drivers of its progress, as it allows patients to undergo procedures without feeling pain (analgesia) or anxiety (due to unconsciousness), nor having memory of the surgical procedure (amnesia).

Despite these considerations, the molecular mechanism by which anesthetics exert their action is still not fully understood and remains an active subject of study: over the years, several hypotheses have been proposed by the scientific community. Initially, the so-called “lipid theory” had a substantial support, according to which anesthetics, being lipophilic drugs, would exert their action by penetrating biological membranes and thereby altering its physical-chemical characteristics and permeability. Most recently, the currently widely accepted hypothesis is the ion channel and protein theory, which suggests that the mechanism by which anesthetics act is related to their interaction with ion channels on the membrane of nerve cells as well as their interaction with receptors, that allosterically influence ion channels. Supporting this hypothesis, it has been demonstrated that some drugs interact with increased affinity with the gamma-aminobutyric acid type A receptor (GABA<sub>A</sub> receptor). The latter is an ion channel that adopts an open conformation when activated by its agonist (gamma-aminobutyric acid, or GABA), allowing chloride ions to enter the neuron and causing hyperpolarization, resulting in an inhibitory effect. Indeed, GABA is the most important inhibitory neurotransmitter in the central nervous system. General anesthetics have been found to be positive allosteric modulators of GABA<sub>A</sub>R and alter its conformation, thereby increasing the probability that GABA will bind to the receptor, enhancing its inhibitory effects.

The present thesis investigated the molecular-level behaviour of inhalation anesthetics, in particular Isoflurane, Sevoflurane, and Desflurane, in their interaction with the GABA<sub>A</sub> ion channel in complex with its ligand, GABA. To this end, molecular models of the Human GABA<sub>A</sub> receptor alpha1-beta2-gamma2 subtype, in complex with GABA, have been created and subsequently simulated together with the phospholipid bilayer through molecular dynamics (MD) simulations. Simulations have been performed in the absence and in the presence of volatile anesthetics, using a flood MD approach. Simulations shed light on the permeation dynamics of anesthetics and allowed to map the binding hotspots of VAs on the receptor, and to study its conformational behaviour. This study lays the groundwork for an improved understanding of how pharmacologically and chemically diverse and clinically essential drugs synergically act to enhance inhibitory signalling in the brain.

# 1. Introduction

*This chapter is a general introduction of the thesis work, providing and summarizing the biological background, the aim and the organization of this research.*

Anesthetics are agents used to induce a reversible loss of sensation or consciousness, so that medical procedures can be performed painlessly. This goal is speculated to be achieved mainly through the depression of neurons in specific areas of the central nervous system, including thalamic neurons, cerebral cortex neurons, GABAergic inhibitory neurons. (C. Wang & Slikker, 2008) Anesthetics can be divided into two major groups: (i) general anesthetics (GA), which induce both loss of sensation and loss of consciousness, and (ii) local anesthetics, which act locally without affecting consciousness. General anesthetics, in turn, can be divided into intravenous anesthetics, administered directly into the bloodstream, and inhalational anesthetics (volatile anesthetics, VA), administered via inhalation.

Despite being widely used in medical practice, the mechanisms of action of anesthetics and their targets are still not fully understood, but the conceptualization of how these drugs reversibly alter central nervous system function has changed over the years. Several research has highlighted the following classes of protein molecules represent the main site of action of anesthetics: ligand-gated ion channels, voltage-gated ion channels, enzymes and carrier proteins. (Bertaccini, 2010) (Franks & Lieb, 1994)

The present work focalises on GABA type A receptor, a ligand-gated ion channel that mediates the inhibitory effects of GABA in the brain, that is considered one of the most significant targets. Volatile anesthetics are thought to enhance GABA<sub>A</sub> receptor activity, increasing chloride ion conductance, hyperpolarizing neurons and reducing excitability.

In this context, Molecular Modeling is very relevant because it gives a tool to study the link between structure and function of molecular machines and the interaction between proteins and small molecules, giving atomistic details which might not be possible to get through experimental techniques alone. (Leach, 2001) Thus, Molecular Modeling is especially advantageous since it allows one to watch conformational movements and protein-ligand interactions that are fundamental to understand their mechanism of action. Furthermore, simulations allow to analyze phenomena at a molecular level on a timescale of nanoseconds or microseconds and spatial scales that are problematic with methods such as NMR or crystallography, thereby saving on the cost of running and waiting for such laboratory experiments. (Hollingsworth & Dror, 2018) Studies on some receptors have demonstrated the potential of modeling in elucidating complex mechanisms, for example Molecular Dynamics simulations have provided information on the allosteric modulation of the Nicotinic Acetylcholine receptor by Volatile

Anesthetics, giving results for designing targeted mutants and confirming hypotheses on the mechanism of action.(Cecchini et al.)

Applying similar techniques, this work analyses in detail the molecular mechanisms responsible for the desirable GABA<sub>A</sub> ion channel modulation by volatile anesthetics, to gain insight into their pharmacological profile and assist in the design of novel, safer, more effective anesthetics.

The work is organized as follows:

**Chapter 1** is the present introduction.

**Chapter 2** provides a biological background on both volatile anesthetics and ion channels. Volatile anesthetics, their critical aspects in clinical application, and their presumed mechanisms of action are briefly described, followed by a short overview of ion channels, particularly those of the 'Cysteine Loop' family.

**Chapter 3** describes the methods used in the present work. An initial description of Molecular Modeling is presented followed by a theoretical discussion of Molecular Mechanics and the Principal Component Analysis.

**Chapter 4** focuses on the study of the interaction between the GABA<sub>A</sub> ion channel in complex with GABA and the volatile anesthetic agents desflurane, isoflurane and sevoflurane. The results of molecular dynamics simulations are analyzed, focusing on possible sites of coherent interaction and local structural alterations.



## 2. Biological Background

### 2.1 An Introduction to Volatile Anesthetics (VAs)

The term anesthesia refers to the total and reversible suppression of pain perception and the absence of reflex response at the same time. If this practice is accompanied by the abolition of consciousness, it is called general anesthesia, while if it concerns specific areas or regions of the body, it is called local anesthesia. The components of modern general anesthesia are three: hypnosis, muscle relaxation, and analgesia, intended not only as the lack of perception of the stimulus, but also as the abolition of the response to pain.

General anaesthetics (GAs) have been in use since the mid-19th century. In 1846, ether anesthesia was introduced into surgery by dentist William W. Morton at University Hospital in Boston where he demonstrated how surgical operations could be performed in the absence of consciousness, pain, and movements induced by painful stimuli. Barbiturates were first synthesized in 1864 but were used as GAs from 1903. Etomidate, a non-gaseous GA, was introduced in the 1950s. Halothane was first used in the 1960s and, despite the risk of causing liver damage in a small number of patients, it is still on the WHO List of Essential Medicines(WHO Model Lists of Essential Medicines.). In the 1970s, the use of enflurane and isoflurane became more widespread, propofol came on the market in the mid-1980s, and the 1990s saw the rise of sevoflurane and desflurane.(Chau, 2010)

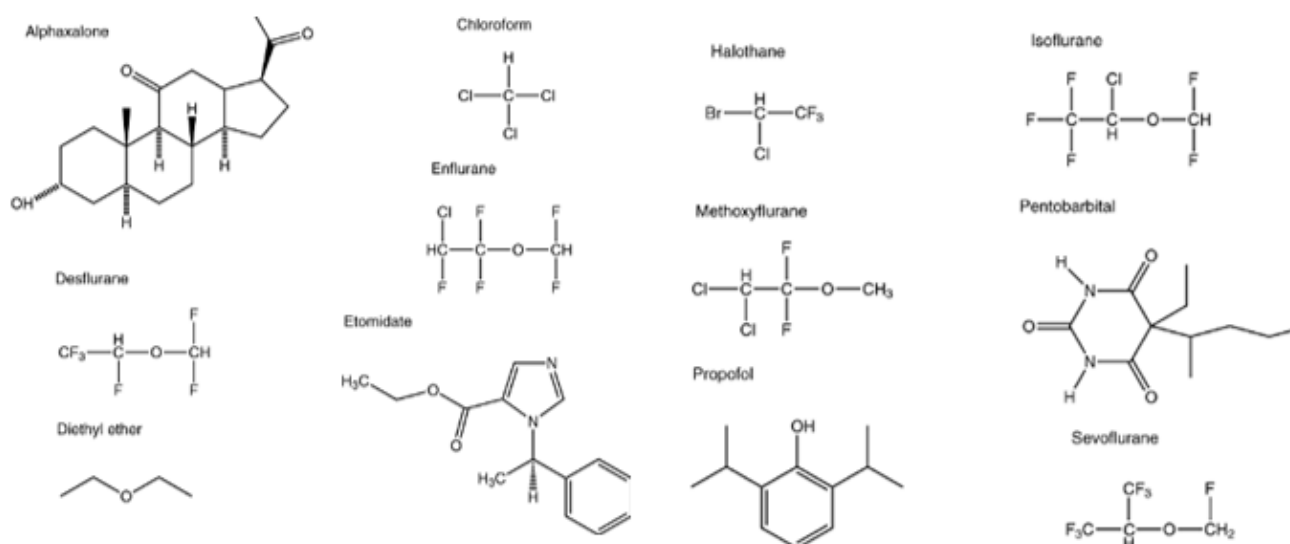


Figure 1- Chemical structures of some common GAs.(C. Wang & Slikker, 2008)

## 2.2 Mechanism of Action

The mechanism of action of anesthesia has been a subject of debate for more than a century, but as time passed, several theories came forward explaining its molecular basis for anesthesia. In the 1870s, Claude Bernard (Bernard, 1870) observed that some agents with very different chemical structures possessed anesthetic activity, which led him to postulate a theory according to which these substances would act through a common mechanism, interfering with the functions of nerve cells, probably by modifying the properties of cell membranes. Approximately 30 years later, Meyer (1899) and Overton (1901) (E, 1991) observed a linear relationship between the potency of anesthetics (in terms of MAC: Minimum Alveolar Concentration required to abolish the response to a painful stimulus in 50% of patients) to induce general anesthesia and their solubility in a lipid-like, non-polar hydrophobic environment (Figure 2). (Campagna et al., 2003) This correlation was measured by the oil/water partition coefficient, a parameter that indicates how much a substance distributes itself between an oily (nonpolar) and an aqueous (polar) solvent. Since neuronal membranes carry signals, and are mostly composed of lipids, anesthetics were assumed to act in lipid areas of brain neuronal surface membranes (Baldassarre et al., 2020). This theory was supported by the noticeable phenomenon known as Pressure Reversal, according to which as ambient pressure increases, the value of MAC also increases. This phenomenon suggests that an increment in ambient pressure compresses the molecules of the system, making the anesthetic less effective because its interaction with the membrane is more difficult. This relationship is remarkably accurate for conventional anesthetics. (Pohorille et al., 1998)

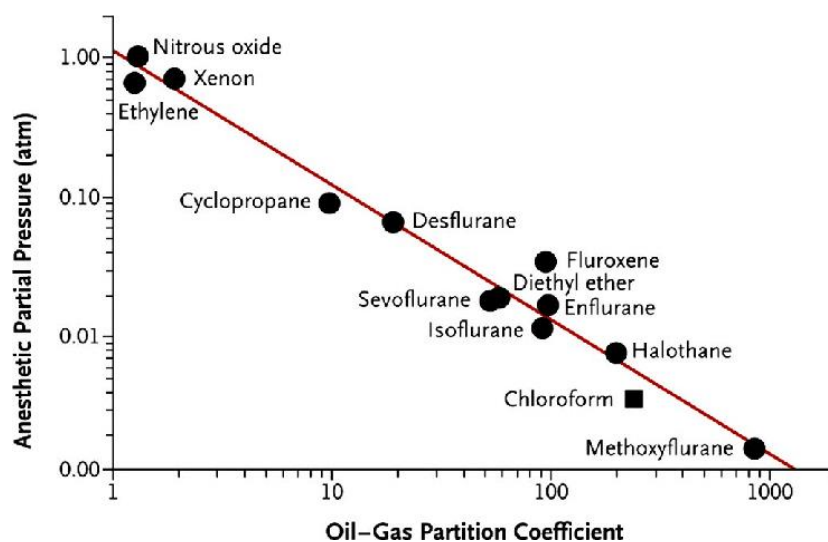


Figure 2-The Meyer-Overton correlation shows the linear relationship between the lipid solubility of anesthetic agents and their efficacy in inducing anesthesia, expressed as anesthetic partial pressure. (Campagna & Forman, 2003)

GAAanesthesia, providing support for the lipid hypothesis. Later, it was realized that this theory alone was not sufficient for understanding the behavior of all anesthetics, as many molecules did not follow this relationship exactly but exhibited a more complex behaviour. For example, some molecules that respect the Meyer-Overton correlation are not anesthetics, while others that violate it are effective.

In 1984, Franks and Lieb found that a water-soluble protein, firefly luciferase, was altered by general anesthetics (Franks and Lieb 1984). This observation led them to postulate the protein theory (Do General Anaesthetics Act by Competitive Binding to Specific Receptors? | Nature.) (Franks & Lieb, 1994), which swiftly garnered widespread approval. The binding of anaesthetics to a hydrophobic pocket on the enzyme molecule inhibits the function of the enzyme in the case of firefly luciferase (Franks et al. 1998). (Antkowiak, 2001)

Once it was speculated that general anesthetics act by binding to a specific site on a protein, efforts were directed at determining which receptors were involved. Starting from their studies (Franks and Lieb, 1984, 1994), Franks and Lieb suggested that ion channels located in the CNS could be relevant targets for anesthetics. A key focus is the gamma-aminobutyric acid A (GABA<sub>A</sub>) receptor. Anesthetics, particularly VAs, appear to impact GABA<sub>A</sub> receptors, with the exception of nitrous oxide and xenon gas anesthetics, which do not influence these receptors. Inhalational anesthetics also have the potential to target glycine receptors and specific potassium channels. Furthermore, there is evidence that inhalational anesthetics competitively bind to N-methyl-D-aspartate (NMDA) receptors, functioning as antagonists.

Ultimately, the mechanism of action of general anesthetics likely involves multiple binding sites. Identifying these sites will enable the development of drugs with more beneficial effects and fewer adverse effects. (Zeiler & Pang, 2024)

## 2.3 Volatile Anesthetics

Inhalation anesthetics are drugs used to induce loss of consciousness, essential for both the induction and maintenance of anesthesia during surgical procedures. They are divided into organic and inorganic anesthetics. The only inorganic anesthetic is nitrous oxide, while organic anesthetics are divided into hydrocarbons and ethers, and the latter further divided into simple and halogenated types. Commonly used halogenated anesthetics are Isoflurane, Desflurane and Sevoflurane. At room temperature, these gaseous anesthetics are in liquid form. They all have a high vapor pressure, which is an indication of the volatility of the anesthetic; therefore, they are easily transformed into vapor by a thermo-compensator, commonly called a vaporizer, which is an integral part of the anesthesia machine.

A given anesthetic induces anesthesia when it achieves an adequate concentration in the brain. In order to reach it, the anesthetic must initially diffuse from alveolar air into the blood and then into the brain. The rate at which this is achieved depends on factors such as the solubility of the anesthetic, its concentration in the inspired air, the rate of pulmonary ventilation, the rate of pulmonary blood flow, and the concentration gradient (partial pressure) of the anesthetic between arterial and venous blood. It is important to mention that inhalation anesthetics distribute among the tissues-or between blood and gases-until equilibrium is established, when the partial pressure of the anesthetic gas in tissues equals that of the inspired gas.

The most widely used scale to assess the potency of inhalational anesthetics is the Minimum Alveolar Concentration (MAC), defined as the minimum concentration required to produce the anesthetic effect, which in 50% of subjects determines the lack of response to a standard noxious stimulus, such as a skin incision (Eger and Saidman 1965). A fraction of the MAC value, around 0.5-0.6 MAC, is sufficient to cause loss of consciousness (MACawake), but a value of approximately 1.3 MAC is necessary to achieve the absence of an autonomic response with the use of inhaled anesthetic alone (MACbar).

Compared to other volatile anesthetics, sevoflurane has several remarkable advantages: a low blood/gas solubility coefficient and a lack of irritating effects on the airways which are also peculiar features of desflurane and isoflurane. This makes it ideal for induction of anesthesia.

Another volatile anesthetic is desflurane, which is used for the induction and maintenance of general anesthesia by inhalation. The chemical structure of desflurane is similar to that of isoflurane but is more stable and less soluble. It is stored at room temperature between 15 and 30°C. The main advantages of desflurane are its low blood/gas solubility coefficient (0.42), which allows to have a precise anesthesia control, and fast induction and recovery. Additionally, only 0.02% of the drug is metabolized, further reducing the possibility of toxicity.

Isoflurane represents one of the most frequently used volatile anesthetics in clinical practice; it is a chemical derivative of fluor chlorinated ether that possesses high chemical stability, and which safety has been well investigated. Isoflurane has an average blood/gas solubility coefficient of 1.4, which provides clinically acceptable induction and recovery times, slower than those of desflurane or sevoflurane. This is a very potent agent with a MAC of approximately 1.15%, making it effective even at low concentrations. The less desirable characteristics of isoflurane are its pungent and irritating action on the airways, tending to provoke cough and bronchospasm, which makes it less suitable for

rapid induction. Although isoflurane is metabolically degraded by a small percentage (about 0.2%), it remains one of the most extensively used anesthetics due to its good balance among efficacy, safety, and cost.

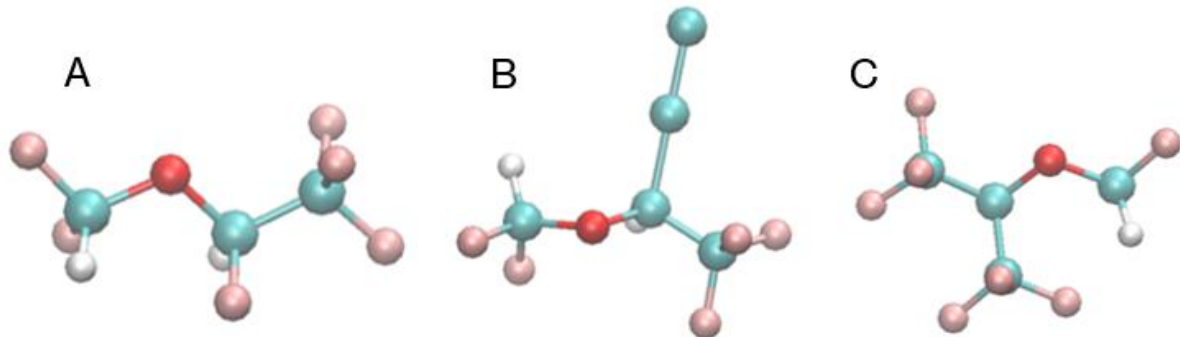


Figure 3- Molecules of Desflurane (A), Isoflurane (B), Sevoflurane (C). Source: Molecular Operating Environment (MOE)

## 2.4 Ion Channels

Some cells, typically known as excitable cells, are specialized for their ability to generate and transmit electrical signals. Although there are many different types of excitable cells, they all use ion channel receptors to convert chemical or mechanical messages into electrical signals. Examples of these include neurons, muscle cells, and contact receptor cells. (Ion Channel | Learn Science at Scitable.)

Ion channels are transmembrane proteins that regulate the passage of specific ions across the plasma membrane, causing rapid changes in membrane potential. The opening of these channels allows ions to flow along their electrochemical gradient, which depends both on the difference in ion concentration between the inside and outside of the cell (chemical gradient) and on the distribution of electrical charges on the two sides of the membrane (electrical gradient). These changes are the basis for the generation and propagation of the action potential, which is the electrical signal that allows communication between excitable cells.

In many studies it has been seen that the ion channels of the central nervous system (CNS) are probable targets for volatile anaesthetics. (Herold & Hemmings, 2012) Ion channels of the “cysteine loop” neurotransmitter receptor family are the most common targets of volatile anesthetics at concentrations used in clinical practice. These receptors function as allosteric signal transducers across the plasma membrane: upon binding of one or more neurotransmitter molecules to an extracellular site, the receptors undergo complex conformational transitions that determine the transient opening of an intrinsic transmembrane channel. (Hassaine et al., 2014) This family includes receptors such as nicotinic acetylcholine, serotonin type 3, GABA<sub>A</sub>, and glycine receptors, as well as glutamate receptors

like NMDA (N-methyl-d-aspartate) and AMPA ( $\alpha$ -amino-3-hydroxy-5-methyl-4-isoxazolepropionic acid).(Howard et al., 2014) Within synapses, these ion channels can affect neurotransmitter release from the presynaptic neuron and alter postsynaptic responsiveness to neurotransmitters. Additionally, voltage-gated sodium, potassium, and calcium channels may be affected by some inhaled anesthetics, though this generally requires higher concentrations than those used clinically(Franks & Lieb, 1994). The current hypothesis is that inhaled anesthetics enhance the activity of inhibitory postsynaptic channels (such as GABA<sub>A</sub> and glycine receptors) and reduce the activity of excitatory synaptic channels (like nicotinic acetylcholine, serotonin, and glutamate receptors)(Campagna et al., 2003). Much of the research has focused on the effects of anesthetics on GABA<sub>A</sub> receptors.

The following is a presentation (Figure 4) of the receptors of the “Cysteine loop” family, with particular attention to the GABA<sub>A</sub> receptor.

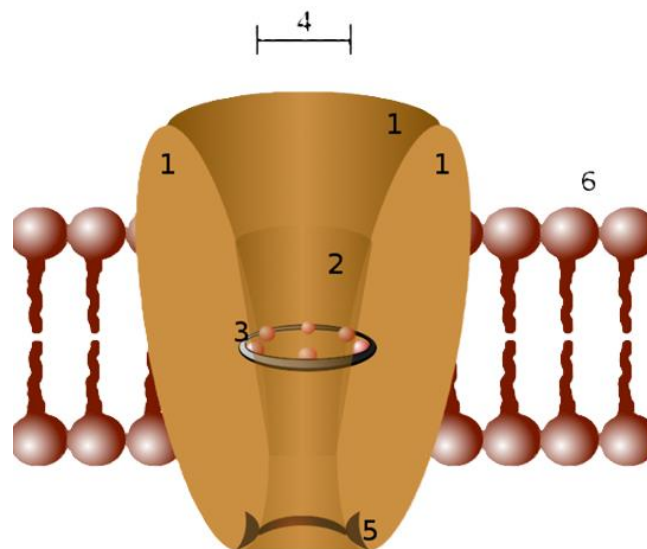


Figure 4- Schematic representation of an ion channel: 1 - protein subunits, 2 - external vestibule, 3 - selective filter, 4 - diameter of the selective filter, 5 - phosphorylation site, 6 - cell membrane. Source: wikipedia

### 2.4.1 Nicotinic Acetylcholine Receptor

Nicotinic acetylcholine receptors, abbreviated as nAChRs are cholinergic receptors which are ligand-gated ion channels in the plasma membrane of some neurons and in the postsynaptic portion of the neuromuscular junction. Binding of acetylcholine to the nicotinic receptor causes a conformational change that opens the ion channel associated with the receptor. This channel allows the cations such as sodium (Na<sup>+</sup>) and potassium (K<sup>+</sup>) to pass through the postsynaptic membrane, according to their electrochemical potential. Some volatile anesthetics such as desflurane, isoflurane and sevoflurane,

can bind to specific sites on the nicotinic receptor and stabilize the receptor in a less reactive or inactive state. This leads to a reduction in the flow of  $\text{Na}^+$  and  $\text{K}^+$  through the channel and, consequently, to postsynaptic depolarization reduction. This is one of the mechanisms that contributes to the depressant effect on the central nervous system, reducing the neuronal activity and leading to unconsciousness and insensitivity to pain.

Functional nicotinic acetylcholine receptors are formed by the combination of five subunits, symmetrically arranged to enclose a pore along which the ion flow occurs. In vertebrates, nicotinic receptors are roughly divided into two subtypes, based on the main location of expression: neuronal NN type nicotinic receptors and muscular NM type nicotinic receptors. The most common neuronal nicotinic acetylcholine receptors are heterologous pentamers of  $\alpha 4\beta 2$  subunits (brain) or  $\alpha 3\beta 4$  subunits (autonomic ganglia). Another class of neuronal receptors in the central and peripheral nervous system is the homomeric  $\alpha 7$  receptor. Muscle receptor subtypes include  $\alpha\beta\delta\gamma$  (embryonic) or  $\alpha\beta\delta\epsilon$  (adult) subunits.(Tassonyi et al., 2002) Depending on the composition of the various subunits, there is a different modulation by the anesthetics. Specifically, in one study (Flood et al., 1997 , Violet et al., 1997 ) it was observed that the nAChR receptors formed by the  $\alpha 4\beta 2$  subunits, are more inhibited by the volatile anesthetic isoflurane at concentrations below the clinical ones. This means that in the presence of isoflurane, these receptors bind less to acetylcholine, reducing the flow of ions through the channel. It suggest that this receptor is highly sensitive to the anesthetic. In contrast, homomeric  $\alpha 7$  receptors are insensitive to isoflurane at clinical concentrations but are inhibited at higher concentrations. Another important aspect is that neuronal nAChRs are inhibited much more potently than muscle nAChRs, which have often served as a model for studying the anesthetic activity of ligand-gated ion channels.(Flood & Role, 1998)

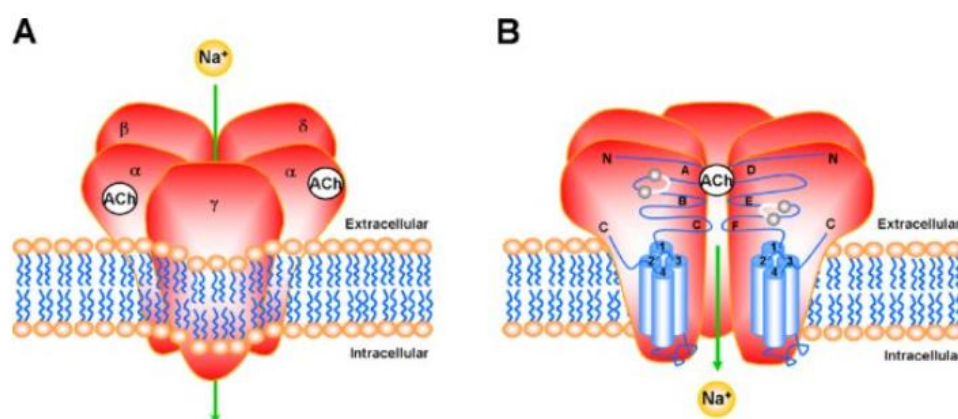


Figure 5- Structure of the nicotinic acetylcholine receptor (nAChR). (A) The five subunits that compose the nAChR receptor are arranged around a central channel, permeable to cations such as  $\text{Na}^+$ . (B) Schematic representation of the heteromeric nAChR receptor in an open state.(Flood & Role, 1998)

## 2.4.2 Serotonin Type 3 Receptor

Serotonin receptors are found on cell membranes of the central and peripheral nervous system and in other cell types and are the sites of action of a variety of drugs and narcotics, including many antidepressants, antipsychotics, and hallucinogens. They regulate both excitation and inhibition of synaptic transmission and are activated by the neurotransmitter serotonin, which is their natural ligand. (Frazer & Hensler, 1999) In contrast to all the other serotonin receptors, which are G proteins coupled, the 5-HT<sub>3</sub> receptor is an ionotropic receptor-channel, directly permeable to sodium (Na<sup>+</sup>) and potassium (K<sup>+</sup>) ions and has a structure like the nicotinic cholinergic receptor. Its activation is due to the binding of the neurotransmitter serotonin (5-hydroxytryptamine, 5-HT) to the extracellular site of the receptor, which triggers a rapid conformational change that opens the channel and allows the passage of ions, depolarizing the neuronal membrane and increasing cellular excitability. Anesthetics, both general and local, can modulate some of their effects through 5-HT<sub>3</sub> receptors.

Some of the volatile anesthetics can alter the function of the 5-HT<sub>3</sub> receptor, enhancing its ionic current and stabilizing the open configuration of the receptor, which enhances the flow of ions and neuronal depolarization. This contributes to the sedation effects, but also to side effects such as post-operative nausea. (Russell & Kenny, 1992) Local anesthetics, though, can inhibit 5-HT<sub>3</sub> receptor action through a blockade by the channel and a reduction of release of the neurotransmitter. This makes 5-HT<sub>3</sub> a valuable target to balance efficacy and side effect in anesthesia.

## 2.4.3 Glycine Receptor

The GlyR is an ionotropic receptor for the amino acid neurotransmitter glycine, with a high prevalence in the spinal cord and brainstem. A peculiarity of these receptors is that the subunit composition can both change during development and in the adult.

The glycine receptor is a macromolecular complex composed of a combination of two homologous subunits  $\alpha$  ( $\alpha$ 1-3) and  $\beta$ . The quaternary structure of the receptor consists of five subunits that are arranged pseudo symmetrically to form a central ion channel. (Admin, 2024)

Glycine binding opens the integral anion channel GlyR and the consequent influx of Cl<sup>-</sup> ions hyperpolarizes the postsynaptic cell, thus inhibiting neuronal activation. Recent studies have shown that volatile anesthetics and ethanol can modulate the activity of GlyR through interaction with the transmembrane domains of the  $\alpha$ 1 subunit. Mihic et al. (1997) (*Sites of Alcohol and Volatile Anaesthetic Action on GABA<sub>A</sub> and Glycine Receptors* | *Nature*) demonstrated that the anesthetic



potentiating action on GlyR is mediated by a critical region of 45 amino acid residues located between the TM2 and TM3 transmembrane domains. These results suggest that anesthetics exert their action by directly binding to specific sites in GlyR, causing allosteric effects that alter its functionality. This type of evidence reinforces the hypothesis of a selective action of anesthetics on inhibitory receptors, contributing to the understanding of their molecular effects in the context of inhibitory neurotransmission.

#### 2.4.4 GABA and GABA<sub>A</sub> Receptor

Gamma-aminobutyric acid (GABA) is the primary mediator of inhibitory GABAergic neurotransmission in the mammalian brain and plays a crucial role in regulating numerous behavioural and emotional functions. It is abundant in the central nervous system (CNS), in particular in the hypothalamus, the basal ganglia, the periaqueductal gray matter and the hippocampus, where it is able to regulate neuronal excitability and muscle tone. (McCormick, 1989) GABA is an endogenous molecule that is produced by our own organism starting from glutamic acid, which is decarboxylated by the enzyme glutamic acid decarboxylase (GAD).

Once produced and released, GABA carries out its activities through two distinct mechanisms: on one hand, it is released by a variety of interneurons located in specific spatiotemporal niches within neuronal circuits; on the other, its physiological effects are conveyed through a wide range of receptors. Thus, GABAergic neurotransmission is mediated by two main types of receptors: GABA<sub>A</sub> and GABA<sub>B</sub>, which are often co-localized in GABAergic synapses. The GABA<sub>A</sub> receptor is the principal site of interaction for GABA, through which neurons exert their inhibitory action.

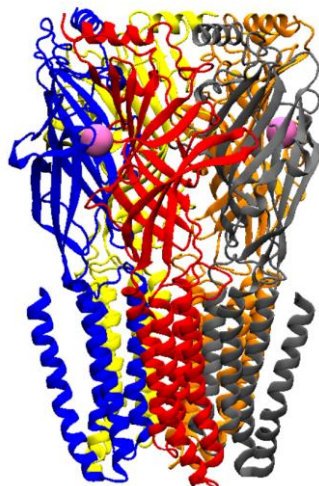


Figure 6- Human GABA<sub>A</sub> receptor alpha1-beta2-gamma2 subtype in complex with GABA (represented with the two pink beads).  
Source: Protein DataBank

GABA<sub>A</sub> receptors are large proteins incorporated in the cell membranes of neurons. Each receptor consists of five subunits that assemble to form a channel at the centre of the complex. Each subunit of the GABA<sub>A</sub> receptor has a large extracellular region located outside the cell membrane, four segments that traverse the cell membrane, and various intracellular regions exposed inside the neuron. While the extracellular protein region is responsible for binding GABA, the intracellular regions can be modified by the addition of phosphate groups. Furthermore, on this receptor complex there are also other specific binding sites for other notable molecules of pharmacological importance capable of modulating the function, such as, for example, benzodiazepines and barbiturates. Many different subunits of the GABA<sub>A</sub> receptor have been identified, which fall into three groups: alpha, beta, and gamma subunits. By combining these subunits in different arrangements, various unique isoforms can be formed. How the subunits organize in the GABA receptor is known for some major isoforms, such as alpha1-beta2-gamma2, but for many other combinations many open questions remain. Structural techniques such as cryo-EM are providing valuable new pieces of information, but there is still much to explore about the formation and regulation of this diversity.(Ghit et al., 2021)

The inhibition induced by GABA<sub>A</sub> receptor activation can occur at both presynaptic and postsynaptic levels. Postsynaptic inhibition, typical of brain neurons (such as those in the cortex, cerebellum, and hippocampus), occurs through membrane hyperpolarization, while presynaptic inhibition, found in the spinal cord, occurs via GABAergic axo-axonic synapses that modulate the excitatory activity of motor neurons. When GABA molecules or similar compounds bind to and activate the receptor, the channel temporarily opens, allowing negatively charged molecules like chloride ions (Cl<sup>-</sup>) to flow from outside the cell to its interior. This ions flow decreases the excitability of the cell. Therefore, compounds that enhance GABA<sub>A</sub> receptor activity cause a greater neuronal inhibition; in contrast, compounds that reduce GABA<sub>A</sub> receptor activity result in the excitation of the neurons receiving the signal.(Mihic & Harris, 1997)

Some anesthetics are very important in this process because they enhance the GABA<sub>A</sub> activity, leading to increased chloride ion flow and membrane hyperpolarization. This improvement of inhibitory activity is essential to anesthetic efficacy, as it contributes to a significant suppression of neural activity and may ensure that the patient remains unconscious during surgery.

## **3. Materials and Methods**

### **3.1 Molecular Modeling**

Molecular Modeling refers to the set of theoretical methods and computational techniques that allow for the modelling of the physical-chemical characteristics and behavior of molecules. Using mathematical models and algorithms, these techniques model the arrangement of atoms, chemical bonds' lengths and angles, torsion angles, and forces between atoms, and enabling many different levels of analysis with atomistic resolution. Several distinct methods belong to the overarching field of molecular modeling, including Quantum Mechanics, which provides detailed electronic information, and Molecular Mechanics, which offers a simplified representation through classical mechanics.

Quantum Mechanics describes the electronic behavior of atoms, chemical properties such as reactivity and energy state based on the Schrödinger equation (Pauling & Wilson, 2012), that describes the movement of electrons in the system. However, with current technology this level of precision is computationally feasible only for small systems, making Quantum Mechanics not useful for large biomolecules.

In contrast, Molecular Mechanics significantly reduces computational effort because it ignores the behavior of electrons and other subatomic particles, treating atoms like point masses, and allowing the study of large systems. Molecular modeling has a wide range of applications, which are rapidly expanding thanks to the increase of computational power and available resources. (Leach, 2001)

### **3.2 Molecular Mechanics**

The term Molecular Mechanics (MM) was coined in the 1970s to describe the application of classical mechanics to determine the equilibrium structure of molecules. It includes a set of theoretical and computational methods to study and predict the structural, dynamic, and thermodynamic properties of molecules and chemical systems. This approach uses Newtonian mechanics and atomic position information to describe a molecular system, facilitating the simulation of systems with many particles. Conceptually, the atoms in a molecule are represented as masses held together by bonds described with harmonic potentials. MM extracts properties, such as energy, of the investigated system by describing it through a potential energy function ( $V$ ) that depends on atomic positions and includes a set of parameters, that together form what is known as the Force Field (FF). Using the force field, simulations can be performed to predict conformations, energies, and molecular dynamics. The main

techniques are molecular dynamics (MD), which simulates molecular movement over time, and Monte Carlo (MC), which explores various configurations to find the one with the minimum energy.

### 3.2.1 Potential Energy Function

The potential energy surface (PES) is a fundamental concept in MM and represents the energy state of the system as a function of its geometry. For a molecular system composed of  $N$  atoms, each identified by a position vector  $r_i$ , the potential energy surface is given by the sum of bonded and non-bonded energy terms:

$$V(r_1, r_2, \dots, r_N) = V_{bond}(r_1, r_2, \dots, r_N) + V_{non-bond}(r_1, r_2, \dots, r_N)$$

Bonded (intramolecular) terms include bond stretching terms, angle bending terms, dihedral (including also improper) terms. Non-bonded (intermolecular) terms are modelled by using the Van der Waals potential and Coulomb electrostatic potential.

$$V_{bonded} = V_{bonds} + V_{angles} + V_{dihedrals}$$

$$V_{non-bonded} = V_{van\ der\ Waals} + V_{electrostatic}$$

These terms refer to variations in internal coordinates or the relative movements of atoms. More advanced force fields might include additional terms, but they always incorporate these fundamental components. (Leach, 2001)

### 3.2.2 Bonded Interactions

As mentioned in the previous paragraph, intramolecular interactions are typically represented as harmonic distortions relative to an equilibrium bond length, bond angle value, and a torsional potential.

The bond stretching term  $V_{bonds}$  represents the interaction between two atoms linked by a covalent bond. The simplest and most widely used model to describe this interaction is Hooke's law, which treats it as a harmonic potential. In this model, the parameters include:

- $k_i$  is the spring constant and indicates the bond's resistance to stretching,
- $l_0$  is the equilibrium bond length, assumed when all other force contributions are zero

- $l_i$  is the actual length of the bond.

$$V_{bonds}(l) = \frac{k_i}{2} (l_i - l_{i,0})^2$$

The harmonic model has also been applied to the angle bending term. It corresponds to a triatomic unit, meaning the angle formed by three atoms when two of them are bonded to the third. This angle can often change uncontrollably, either increasing or decreasing. The parameters of the  $V_{angles}$  formulation are:

- $h_i$  is the angle stiffness,
- $\theta_{i,0}$  is the reference bond angle, when all other force contributions are zero,
- $\theta_i$  is the actual bond angle.

$$V_{angles}(\theta) = \frac{h_i}{2} (\theta_i - \theta_{i,0})^2$$

The torsional term, also called the dihedral term, refers to the rotation of a bond between four atoms (A, B, C, D) that are sequentially bonded. The torsional angle is the angle between the A-B bond and the plane identified by B-C-D atoms (Figure 7). Proper dihedrals refer to a complete rotation, whereas improper dihedrals occur when the rotation is restricted. Due to possible symmetries, where multiple positions correspond to the same energy minimum, the potential energy associated with the dihedral angle follows a sinusoidal pattern, allowing for several possible positions. The parameters are:

- $V_n$  is the torsional stiffness,
- $\gamma$ , is the torsional equilibrium angle and defines the position of the minimum of the function,
- $\phi$  is the dihedral angle when all terms are considered.

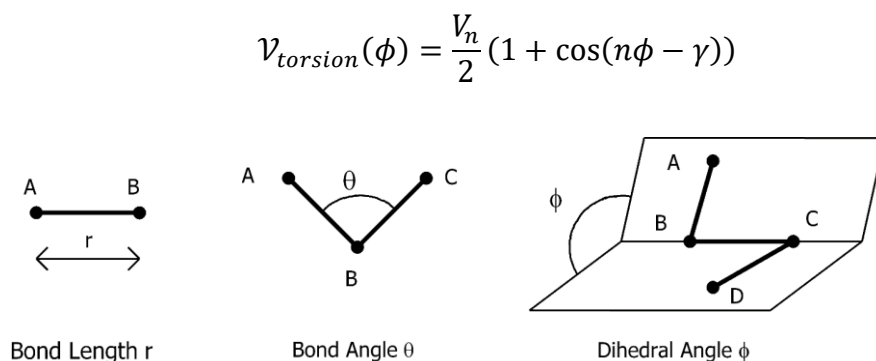


Figure 7- Representation of bond interactions. From left to right: bond length between atom A and atom B; bond angle between atoms A, B, C; and dihedral angle between four atoms A, B, C, D.

### 3.2.3 Non-Bonded Interactions

Non-bonding terms are essential for maintaining the three-dimensional structure of the system and represent the behavior of atoms when they are close enough to influence each other, but without forming bonds. The non-bonding terms are usually modeled as a function that depends on the inverse power of the distance and consist of two components: Van der Waals forces and electrostatic interactions.

Van der Waals interactions consist of attractive and repulsive components, the strength of which varies depending on the distance between the atoms. At very short distances, a repulsive force dominates, which increases exponentially with decreasing distance, and originates from the Pauli exclusion principle. According to this principle, two electrons within the same atom cannot share the same quantum state, preventing the overlap of electron clouds of neighbouring atoms and thereby generating repulsion between the nuclei. In contrast, at larger distances, attractive interactions become predominant, mainly due to the London dispersion force. This is a weak intermolecular force that occurs when electrons in adjacent atoms, due to their instantaneous positions, form temporary dipoles, inducing opposite dipoles in neighboring atoms and causing an attraction also known as induced dipole attraction. Therefore, Van der Waals forces are essential to understanding the molecular behavior of systems, especially when there are no other types of interactions or are limited.

$$V_{vdW}(r_{ij}) = 4\epsilon_{ij} \left[ \left( \frac{\sigma_{ij}}{r_{ij}} \right)^{12} - \left( \frac{\sigma_{ij}}{r_{ij}} \right)^6 \right]$$

Where:

- $V(r)$  is the interaction potential as a function of the distance  $r$  between the two particles.
- $\epsilon$  is the well depth that measures the strength of the attractive interaction.
- $\sigma$  is collision diameter which represents the value of  $r$  at which the potential is zero (i.e., the point where the attractive and repulsive forces balance each other).

In particular, the term  $\left( \frac{\sigma_{ij}}{r_{ij}} \right)^{12}$  describes the short-range repulsive component of the interactions, while the term  $\left( \frac{\sigma_{ij}}{r_{ij}} \right)^6$  represents the long-range attractive component, associated with London dispersion forces. This function provides a good approximation for modelling non-bonded interactions in a wide range of physical and chemical systems.

Electrostatic interactions are fundamental forces that act between charged particles and are present even at distances greater than a nanometer. Despite their spatial extension, these interactions still exert a significant influence, thus requiring considerable computational effort to be accurately modeled. These interactions are generally described by the Coulomb Potential, expressed as:

$$V_{electrostatic}(r_{ij}) = \frac{q_i q_j}{4\pi\epsilon_0 r_{ij}}$$

where:

- $r_{ij}$  is the distance between atoms,
- $q_i$   $q_j$  are the charges of atoms,
- $\epsilon_0$  is the dielectric constant.

The calculation of non-bonded interactions between particles can be computationally expensive, because they are proportional to the square of the number of particles  $N$ . To address this complexity, various methods have been developed to reduce computational costs. One particularly effective strategy is the use of a cutoff. By applying a cutoff value, interaction calculations are limited to only those atom pairs whose distance is below this predefined threshold. This approach effectively excludes interactions that occur beyond the cutoff, significantly reducing the number of required calculations and improving simulation efficiency. In addition to the cutoff method, additional optimization techniques (i.e. Switched Potentials) have also been proposed to further simplify the calculation of nonbonded interactions and to balance accuracy and computational performance, allowing for more manageable and precise simulations. (Notman & Anwar, 2015)

$$\begin{aligned}
U = & \sum_{i<j} \sum 4\varepsilon_{ij} \left[ \left( \frac{\sigma_{ij}}{r_{ij}} \right)^{12} - \left( \frac{\sigma_{ij}}{r_{ij}} \right)^6 \right] \\
& + \sum_{i<j} \sum \frac{q_i q_j}{4\pi\varepsilon_0 r_{ij}} \\
& + \sum_{\text{bonds}} \frac{1}{2} k_b (r - r_0)^2 \\
& + \sum_{\text{angles}} \frac{1}{2} k_a (\theta - \theta_0)^2 \\
& + \sum_{\text{torsions}} k_\phi [1 + \cos(n\phi - \delta)]
\end{aligned}$$

Figure 8- Potential energy function contributions. The first and the second terms represent the non-bond interactions: respectively, the van der Waals potential modelled by Lennard-Jones 12-6 equation, and the electrostatic potential modelled by Coulomb's law. (Notman & Anwar, 2015)

### 3.2.4 Periodic Boundary Conditions

To accurately calculate potential energy in simulations of physical systems, it is essential to correctly set the boundary conditions to avoid artifacts from long-range interactions. These systems, whose number of particles is finite, are enclosed in a unit cell that can have the shape of a cube, parallelepiped, prism, hexagon, truncated octahedron or rhombic dodecahedron. This confinement can lead to problems because particles near the cell boundaries behave differently from those at the center, due to edge effects. To solve this problem, periodic boundary conditions (PBC) are used, which create a seemingly infinite system by surrounding it with identical copies of itself. This method ensures that particles near the edges interact as if they were inside a larger, continuous system, thus improving the realism of the simulation.

A key aspect of this approach is that to avoid artifacts, each particle must not interact with its own replica in adjacent unit cells. Therefore, the unit cell size must be carefully chosen so that the distance between any particle and its closest replica exceeds the threshold set for non-bonded interactions. GROMACS implements the Minimal Image Convention to ensure that each particle interacts only with the closest particle within the unit cell. As illustrated in (Figure 9) when a particle crosses a cell boundary, it is replaced by an identical particle from an adjacent cell, maintaining a seamless simulation and improving result accuracy. Additionally, repeating the cell in all spatial directions ensures a constant number of atoms within the simulation box.



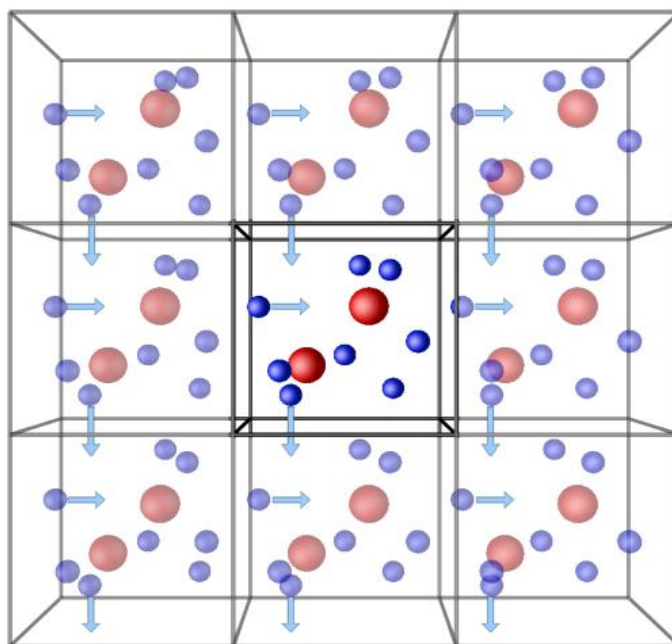


Figure 9- Schematic representation of the idea of periodic boundary conditions for a cubic box. Source: <http://isaacs.sourceforge.net/phys/abc.html>

### 3.2.5 Potential Energy Minimization

The search for stable states of a molecular system, corresponding to minimum energy configurations of the atoms, plays a crucial role in Molecular Modeling, especially in conjunction with Molecular Dynamics simulations. This process, commonly referred to as optimization, is central not only in computational chemistry but also in various other engineering fields, as it involves the problem of minimizing potential energy, regardless of its mathematical representation. (Schlick, 2010)

The potential energy surface (PES) is a multidimensional function that depends on the coordinates of the molecular system. For a system of  $N$  atoms, the PES is characterized by  $3N$  Cartesian coordinates or  $3N-6$  internal coordinates, which include parameters such as bond lengths, bond angles, and torsion angles. Due to its inherent complexity, PES can only be easily visualized for very simple systems. Molecular mechanics (MM), using computational methods, focuses on identifying minima on the potential energy surface, since these represent energetically favorable states and stable configurations of the system. Therefore, energy minimization allows to obtain a stable configuration, in which atomic collisions are avoided, and serves as a fundamental preliminary step before proceeding with more advanced simulations.

In general, the energy surface is characterized by stationary and saddle points. Stationary points usually correspond to local or global minima, representing stable configurations of the system. Saddle points, on the other hand, are the highest points between the minima and represent transition states, so

configurations through which the system can pass from one energy minimum to another. Typically, starting from an initial configuration does not lead to the discovery of the global minimum. Most algorithms are only able to find the local minimum closest to the starting point. There are various approaches used to find a local minimum, which are classified into (i) derivative methods and (ii) non-derivative methods. The former require the calculation of the energy function's derivatives with respect to the system's coordinates to guide the search for the minimum, while the latter are geometric methods. An example of a non-derivative minimization method is the Simplex method, which is based on constructing a geometric figure with  $N+1$  interconnected vertices, where  $N$  is the dimensionality of the energy function being considered. Each vertex corresponds to a specific set of coordinates for which an energy value can be calculated. For a 2D function, the figure is a triangle; for a 3D function is used a tetrahedron. The position of the vertex, corresponding to a given energy value, is adjusted at each step through movements such as reflection, reflection and expansion, or reflection and contraction of the figure. This process continues until a vertex with sufficiently low energy is found. The Simplex method works well when the energy is relatively high but becomes less and less accurate when the search approaches the minimum.

Derivative methods, in turn, are divided into first order and second order methods. First-order methods (e.g., Steepest Descent(Fletcher & Powell, 1963) and Conjugate Gradient(McCarthy, 1989)) use the gradient, or first derivative of the potential energy function to move toward a minimum: the direction indicates where the minimum is, and the magnitude indicates the steepness of the local slope. As a result, the atom coordinates change as the algorithm moves the system toward the minimum, and the final configuration of a step becomes the starting point for the next iteration. Second-order methods (e.g., Newton-Raphson(The Newton-Raphson Method: International Journal of Mathematical Education in Science and Technology: Vol 26 , No 2 - Get Access) and L-BFGS(A Broyden—Fletcher—Goldfarb—Shanno Optimization Procedure for Molecular Geometries - ScienceDirect)) use both first and second derivatives, which provide information about the curvature of the function that allows to understand where the potential energy function will change direction. The latter are more accurate but require more computational effort. In general, each method has its advantages and disadvantages, and the choice depends on the nature and characteristics of the considered system.

### 3.3 Molecular Dynamics

Molecular Dynamics is one of the main areas of interest of Molecular Mechanics and is a set of computational simulation techniques that, through the integration of the equations of motion, allows to study the evolution dynamics of systems.

Simulation techniques are playing a significant role in the field of protein engineering and drug discovery, as they allow to study chemical and biological processes, predict protein properties, and analyze interactions between small molecules and macromolecules. Thanks to significant improvements in speed, accuracy and the amount of available data, today these simulations permit to capture the dynamic behavior of biomolecules in greater detail and with an extremely fine time scale. Furthermore, Molecular Dynamics simulations have proven to be a fundamental step also for discovering the structural basis of diseases and designing therapeutic molecules. (Hollingsworth & Dror, 2018)

Molecular dynamics consist of the resolution of Newton's laws of motion for every particle in the system. The law of motion for N particles with mass  $m_i$  and position  $x_i$  can be written as:

$$m_i \frac{\partial^2 x_i}{\partial t^2} = F_i$$

Or, alternatively in matrix form:

$$M\ddot{X}(t) = F(X)$$

with M being the diagonal mass matrix,  $\ddot{X}(t)$  the acceleration vector and F(X) the collective force. The latter is usually expressed as a function of potential energy:

$$F(X) = -\nabla E[X(t)]$$

where  $\nabla E[X(t)]$  is the vector of first derivatives of the potential energy with respect to the position of the particles,  $x_i$ :

$$\nabla E(X)_i = \frac{\partial E(X)}{\partial r_i}$$

with  $r_i$  representing one directional component of a given particle. Since these equations are generally not solvable analytically for larger systems, they are solved numerically, yielding a trajectory of positions and velocities.

### 3.3.1 Statistical Ensemble

The microscopic state of a system is defined by the atomic positions  $r$  and momenta  $p$ ; these coordinates exist in a multidimensional space called phase space (or state space). A single point in the phase space describes the state of the system at a given moment, and the collection of points that satisfy the conditions of a particular thermodynamic state forms the thermodynamic ensemble.

By definition, a statistical ensemble is a set of all possible systems that, while having different microscopic states (i.e., different configurations of  $r$  and  $p$ ), share the same macroscopic or thermodynamic state. This concept is fundamental in statistical mechanics, where ensembles are used to describe the average properties of a system, such as energy, pressure, or temperature, without having to track every individual particle trajectory.

Statistical Ensemble	Constants
Canonical	N, V, E
Isothermal-Isobaric	N, V, T
Gran Canonical	$\mu$ , V, T
Microcanonical	N, p, T

*Table 1- The different statistical ensembles. The Canonical ensemble (NVE) is an isolated system in which volume (V), energy (E) and number of particles (N) are fixed. The Isothermal-Isobaric ensemble (NVT) is a closed system characterised by fixed number of particles (N), volume (V) and temperature (T). The Gran-Canonical ensemble ( $\mu VT$ ) corresponds to an open system where chemical potential ( $\mu$ ), volume (V) and temperature (T) are kept constant. In the Microcanonical ensemble (NpT) the fixed characteristics are the number of particles (N), pressure (P) and temperature (T).*

By integrating over all possible configurations of a system, it is possible to obtain the representative properties of all microstates belonging to a single macrostate. This operation leads to the Ensemble Average, which is given by:

$$\langle A \rangle_{ensemble} = \iint A(p^N, r^N) \rho(p^N, r^N) dp^N dr^N$$

where  $A(p^N, r^N)$  is the property of interest, expressed as a function of momenta  $p$  and positions  $r$ , and  $\rho(p^N, r^N)$  is the probability density of the ensemble, which in turn is defined as:

$$\rho(p^N, r^N) = \frac{1}{Q} \exp \left[ -\frac{E(p^N, r^N)}{k_B T} \right]$$

where  $k_B$  is the Boltzmann's constant,  $T$  is the temperature,  $Q$  the partition function, and  $E(p^N, r^N)$  the energy.

The partition function  $Q$  for the Canonical Ensemble is given by:

$$Q = \iint \exp\left[\frac{-H(p^N, r^N)}{k_B T}\right] dp^N dr^N$$

The partition function  $Q$  is defined as the sum of all the energies of the system and to determine it it is necessary to know all the possible physical states of the system, therefore it is very difficult to calculate it analytically. For this reason, the ergodic hypothesis is accepted. According to this hypothesis, the ensemble average of a physical property is equal to the time average of the same property, provided it is observed over a sufficiently long period. The time average of a property  $A$  over the duration of the measurement is given by:

$$\langle A \rangle_{time} = \lim_{\tau \rightarrow \infty} \frac{1}{\tau} \int_{t=0}^{\tau} A(p^N(t), r^N(t)) dt$$

According to the ergodic hypothesis:

$$\langle A \rangle_{ensemble} = \langle A \rangle_{time}$$

In this way it is easier to consider the average properties of the system and its microscopic properties, which are obtained with a sufficiently long simulation and provide a realistic representation of the 'real' dynamics of molecular systems. (Skeel, 2009)

### 3.3.2 Molecular Dynamics Software

Several software packages are designed to perform molecular dynamics simulations, each with its own specific features and applications; among these are: AMBER, CHARMM, NAMD, GROMACS.

GROMACS (GRONingen MACHine for Chemical Simulations) initially developed by the University of Groningen and subsequently supported and improved by other institutions, is one of these most widely used pieces of software. The goal of GROMACS is to provide a versatile and efficient MD program for the simulation of biological (macro) molecules in aqueous and membrane environments, and capable of running on single processors as well as on parallel computer systems. It stands out for its efficiency in handling large-scale systems, thanks to several optimization techniques that

surprisingly increase the computational speed. In addition, the program package includes a wide range of analysis tools (e.g. extended graphical trajectory analysis, principal component analysis, and others) that can be performed on defined or user-selected groups of atoms. (Van Der Spoel et al., 2005) These analyses allow for a more comprehensive view of the trajectories of the systems, making this software a valuable resource for researchers in the field of bioinformatics. (Bauer et al., 2022)

### 3.3.3 Principal Component Analysis

To obtain a concise interpretation of the large amount of Molecular Dynamics simulation data and to try to reduce the description of the molecular motion from  $3N$  atomic coordinates to a few collective degrees of freedom, which take into account the essential dynamics of the system, several analysis strategies have been developed.

Principal Component Analysis (PCA) is a technique used in statistics and has the aim of reducing a high number of variables that describe a set of data to a smaller number of variables called Principal Components (PCs), limiting the loss of information as much as possible. (Tufféry, 2011)

The correlated internal motion of a molecule with  $N$  atoms can be described by a covariance matrix,

$$C_{ij} = \langle (x_i - \langle x_i \rangle) (x_j - \langle x_j \rangle) \rangle$$

where  $x_1, \dots, x_{3N}$  are mass-weighted Cartesian coordinates and  $\langle \dots \rangle$  represents the ensemble average over all sampled conformations. (Sittel et al., 2014)

By diagonalizing this covariance matrix, one obtains  $3N$  eigenvectors ( $e_j$ ) and corresponding eigenvalues ( $\sigma_j^2$ ), which describe the collective motion modes of the system and their respective amplitudes. The eigenvectors define a new coordinate system where each component represents an independent mode of motion, ranked by decreasing variance.

To analyze the motion along a specific mode, the trajectory can be projected onto the corresponding eigenvector, obtaining the principal component projections  $p_j(t)$ , which describe the motion of the system along the principal axes:

$$p_j(t) = [x(t) - \langle x \rangle] \cdot e_j$$

The Mean Square Fluctuation (MSF) is the sum of  $3N$  contributions from the variety of PCs:

$$\langle (x(t) - \langle x \rangle)^2 \rangle = \sum_{j=1}^{3N} \text{var}(p_j) = \sum_{i=1}^{3N} \sigma_i^2$$

This relation highlights that the sum of the eigenvalues represents the total atomic fluctuation of the system. Typically, the first few PCs account for the majority of the system's MSF, capturing the most relevant large-scale motions. In biomolecular systems, only the first few PCs are generally analyzed, as they describe the dominant collective motions while filtering out high-frequency fluctuations that are often less relevant to the functional dynamics.

### 3.3.4 General Force Fields

In molecular dynamics simulations, the parameterization of small molecules, such as ligands, is essential to ensure consistency and accuracy. Since standard force fields developed for proteins and membranes do not directly cover these molecules, general force fields such as the CHARMM General Force Field (CGenFF) for CHARMM-based systems and the General AMBER Force Field (GAFF) for AMBER-based systems are used. These force fields are designed to accurately describe the structural and dynamic properties of a wide range of organic compounds, providing parameters for bonds, angles, torsions, and non-bonded interactions.

CGenFF employs a parametric analogy approach, assigning parameters to ligands based on previously parameterized model compounds within the CHARMM library. This method assigns a penalty score to less reliable parameters, indicating the need for further manual optimization. High penalty scores suggest that additional quantum mechanical simulations may be required to refine values such as torsional energy or partial charges. (Vanommeslaeghe et al., 2010)

GAFF, on the other hand, adopts a more automated approach, based on a reduced number of atom types and an empirical parameter assignment, making it suitable for greater transferability across molecules with diverse structures. The parameter assignment process in GAFF is managed by the Antechamber tool, which automatically identifies ligand atom types and assigns the corresponding GAFF parameters. If some parameters are not directly available, a specific program intervenes to estimate them, ensuring that the resulting parameter set is compatible with the AMBER force field. (J. Wang et al., 2004)

A critical aspect of parameterization concerns the assignment of partial charges, which are essential for accurately describing electrostatic interactions. GAFF employs the AM1-BCC method (Austin Model 1 with Bond-Charge Corrections), a semi-empirical model that starts with charge calculations based on AM1 and applies additive bond charge corrections, calibrated to reproduce the RESP fit used in AMBER force fields. This method allows for reliable charge assignment with reduced computational cost, making it particularly useful for large-scale simulations.

CGenFF, instead, optimizes partial charges to reproduce specific interactions with a water molecule in the gas phase. During the force field development, charges are calibrated to ensure that the dipole moment and interaction energies of an organic fragment with a water molecule match those obtained from quantum mechanical calculations. This approach aims to indirectly incorporate the effects of biological environment polarization, ensuring that electrostatic interactions between the ligand and the protein/membrane are realistic.(Vanommeslaeghe et al., 2012)

The choice between CGenFF and GAFF depends on the force field used for the macromolecule and the trade-off between accuracy and speed. CGenFF provides a more rigorous parameter assignment and allows greater manual control over parameter quality, making it more suitable for ligands with complex or rare functional groups, for which automatically generated parameterization may not be adequate. GAFF, on the other hand, offers high transferability and immediate parameterization, making it an efficient choice for large-scale simulations involving numerous small organic molecules.

Both methods are widely validated and used within the scientific community; the choice primarily depends on the simulation framework and the level of precision required for ligand description.



## 4. Interaction between $\alpha 1\beta 2\gamma 2$ GABA A receptor and Volatile Anesthetics

*This chapter will describe the investigation of ion channels as potential targets of anesthetic action. Specifically, the study examines the interactions and effects of three different volatile anesthetics, desflurane, isoflurane, and sevoflurane, on the GABA<sub>A</sub> ion channel through the use of molecular dynamics simulations.*

### 4.1 Introduction

General anesthetics are a fundamental class of drugs in modern medicine. Their ability to reversibly suppress conscious brain activity, preserving most other physiological functions, makes them indispensable in surgical procedures, but. Despite that, their precise mechanism of action is not completely understood. Over the years, many theories have tried to explain how these compounds exert their effects. Early hypotheses, like the Meyer-Overton correlation, were based on their solubility in lipid environments, whereas more recent theories point to specific molecular targets like ion channels and neurotransmitter receptors. Among these, GABA<sub>A</sub> receptor is one of the most studied targets, due to its crucial role in inhibitory neurotransmission.

GABA<sub>A</sub> receptor is a ligand-gated ion channel that mediates inhibitory synaptic transmission, allowing chloride ion influx and the activation by gamma-aminobutyric acid (GABA). Its modulation by general anesthetics leads to an increase in neuronal inhibition, contributing to the sedative, amnesic, and immobilizing effects characteristic of anesthesia.

In the present work, molecular dynamics (MD) simulations are employed to investigate the interactions between the GABA<sub>A</sub> receptor and three commonly used volatile anesthetics: desflurane, isoflurane, and sevoflurane. These agents have been widely used in clinical practice since the late 20th century due to their efficacy in inducing anesthesia and maintaining unconsciousness, with minimal side effects. Although they share a common mechanism of action, they exhibit distinct pharmacokinetic properties that influence their clinical applications, including differences in solubility, metabolism, and anesthetic potency, in terms of Minimum Alveolar Concentration (MAC).

Desflurane, characterized by its low blood solubility, allows for rapid induction and recovery with more precise control of anesthesia, making it particularly suitable for outpatient procedures. However, it has the highest MAC (~6.0%), meaning that is needed a higher concentration to achieve the desired effect. Sevoflurane, thanks to its low airway pungency and smooth induction profile, is often preferred in pediatric anesthesia and has an intermediate MAC (~2.0%), balancing potency and ease of administration. Isoflurane, although slower induction and recovery times due to its greater solubility in blood, remains a valid option for maintenance of anesthesia in various surgical settings. Its lowest MAC (~1.2%) makes it the most potent of the three, allowing effective anesthesia even at lower concentrations.(R. D. Miller et al., 2014)

By embedding the receptor in a lipid bilayer and simulating its behavior with and without anesthetic molecules, it is possible to characterize their binding sites, assess their impact on receptor conformation, and explore potential allosteric effects that could influence channel function. Previous structural studies have provided insights into the receptor's architecture and its interactions with various modulators, including intravenous anesthetics and benzodiazepines. However, the dynamic and transient nature of volatile anesthetic binding can greatly benefit from atomistic-level computational approaches to complement experimental findings.

## **4.2 Materials and Methods**

As a first step in the present work, a thorough review of existing methodologies for studying ligand-receptor interactions was conducted, with a particular focus on target proteins in computational studies of general anesthetics. While multiple protein targets have been proposed for anesthetic action, such as ion channels, membrane receptors, and cytoskeletal components, the GABA<sub>A</sub> receptor has been chosen as the subject of investigation due to its well-documented role in mediating inhibitory neurotransmission and its established pharmacological modulation by anesthetic compounds.(Olsen & Sieghart, 2009) This pentameric ligand-gated ion channel is a key role in the central nervous system, and its interaction with anesthetics has been implicated in the induction of hypnosis, sedation, and loss of consciousness.(Franks & Lieb, 1994)

Several structural models of the GABA<sub>A</sub> receptor have been resolved using cryo-electron microscopy, each capturing different conformational states and ligand-bound complexes. For the purpose of this study, PDB entry 6X3Z was selected as the structural model, based on multiple considerations: (1) it represents the human  $\alpha 1\beta 3\gamma 2$  isoform, which is the most prevalent form of the receptor in the mammalian brain and the primary target of clinically relevant anesthetics; (2) it provides a high-resolution model in complex with GABA, allowing for the investigation of anesthetic binding in a physiologically relevant conformation; (3) its structural features, including well-defined binding pockets and transmembrane domain organization, facilitate molecular dynamics simulations aimed at identifying preferential interaction sites for volatile anesthetics.

The three-dimensional structure of the human GABA<sub>A</sub> receptor alpha1-beta2-gamma2 subtype in complex with GABA (2 mM GABA) was downloaded in PDB format from the Protein Data Bank (Berman, 2000), using the code 6X3Z. This structure was taken from a previous study, in which structures of GABA<sub>A</sub> receptors bound to intravenous anesthetics, benzodiazepines, and inhibitory modulators were obtained by single-particle electron microscopy at a resolution of 3.23 Å. (Kim et al., 2020)

Overall, GABA<sub>A</sub> is an heteropentamer, consisting of five protein chains that correspond to the five subunits (Table 2).

CHAIN	FIRST RESOLVED RESIDUE	LAST RESOLVED RESIDUE	LENGTH
A subunit beta-2	Ser 7	Val 340	334
B subunit alpha-1	Asp 10	Arg 347	338
C subunit beta-2	Ser 7	Val 340	334
D subunit alpha-1	Asp 10	Arg 347	338
E subunit gamma-2	Gly 62	Leu 394	333
			1677 Residues

*Table 2- Five chains of GABA<sub>A</sub> receptor and number of residues crystallized.*

GABA<sub>A</sub> is reported in complex with its ligand GABA (Gamma-Amino-Butanoic Acid C<sub>4</sub>H<sub>9</sub>NO<sub>2</sub>). There are two GABA molecules, with residue identifier “ABU”, that bind to the A and C chains that

represent the beta-2 subunits. This complex was immersed in composite asymmetrical lipid patch representative of the mammalian cell membrane, used in several studies (Zizzi et al., 2022), composed of POPC (1,2-palmitoyl-oleoyl-sn-glycero-3-phosphocholine), POPE (1-Palmitoyl-2-oleoyl-sn-glycero-3-phosphoethanolamine), POPS (1,2-palmitoyl-oleoyl-sn-glycero-3-phosphoserine), PSM (palmitoylsphingomyelin) and Cholesterol (CHOL). The numbers of different lipid molecules in the two leaflets of the membrane are shown in the table below (Table 3).

<b>LIPID</b>	<b>INNER LEAFLET</b>	<b>OUTER LEAFLET</b>	<b>TOTAL</b>
POPC	40	106	146
POPE	132	34	166
POPS	82	8	90
PSM	10	116	126
CHOL	136	136	272
<b>Total</b>	400	400	800

*Table 3- Number of lipid molecules in the two sheets of the membrane model.*

The molecular structures of the volatile anesthetics Desflurane, Isoflurane and Sevoflurane (Figure 10) in mol2 format, were obtained using the Molecular Operating Environment (MOE)(*Molecular Operating Environment (MOE) | MOESaic | PSILO*) software, a platform for chemical calculation and molecular modeling. The mol2 files contain information about their chemical structure (atoms, their positions in space and bonds) and report the correct protonation state of the molecules. The partial charges and protonation states were calculated using MOE 2022 with the AM1-BCC method, improving accuracy in reproducing electrostatic interactions relevant for molecular simulations.

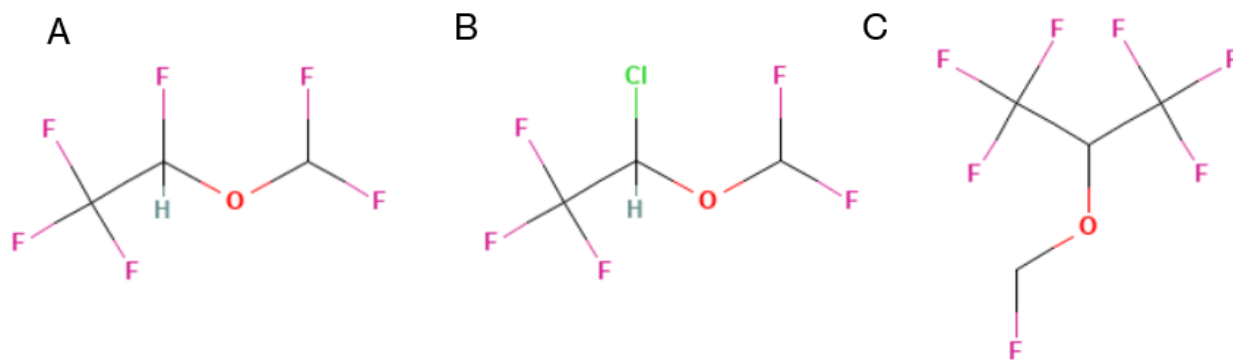


Figure 10- 2D representation of Desflurane (A), Isoflurane (B), Sevoflurane (C) molecules.

Subsequently, using the CGenFF (CHARMM General Force Field)(faadmin.) software, the topologies and force parameters of the molecules were generated in CHARMM(Vanommeslaeghe et al., 2010) format, which were then transformed into a GROMACS compatible format through the script `cgenff_charmm2gmx.py`, downloaded from the MacKerell lab website with the latest CHARMM36 force field tarball. This script allows to obtain in output: (i) the .itp file that contains the topology of the molecule converted to GROMACS format; (ii) the .prm file that includes the parameters (bonds, angles, impropers, etc.) translated into GROMACS; (iii) the .top file that is the GROMACS topology that includes the .itp and .prm files; (iv) the .pdb file that contains the coordinates of the molecule in PDB format, generated from the .mol2 file.

Finally, the ligand parameters were merged with the receptor structure, appropriately modified.

### 4.2.1 Model building

The structure of the GABA<sub>A</sub> receptor in complex with its neurotransmitter (6X3Z) was embedded in the membrane model described above and the systems were assembled using the Membrane Builder(*CHARMM-GUI Membrane Builder toward Realistic Biological Membrane Simulations - Wu - 2014 - Journal of Computational Chemistry - Wiley Online Library*) tool of CHARMM-GUI(Jo et al., 2008). A system pH of 7 was imposed, and glycans have been omitted for simplicity. The model was oriented along the Z-axis and translated by -35 Angstroms, to ensure that the GABA<sub>A</sub> alpha helices are the transmembrane portion. To ensure adequate hydration of the lipids, the explicit TIP3P water model has been used to solvate the rectangular simulation box and the water thickness was set to 50, indicating the minimum height of the water at the top and bottom of the system. In addition, a physiological NaCl concentration of 0.15M was inserted into the system.

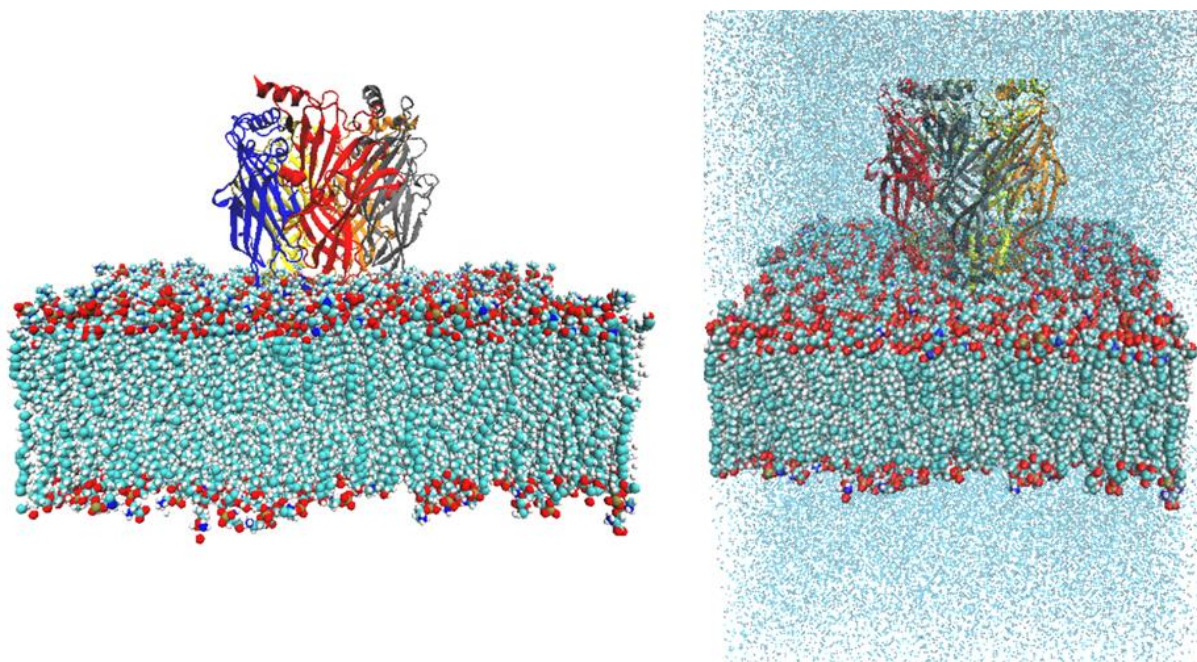


Figure 11- Model of a membrane-embedded GABAA ion channel. Source: CHARMM-GUI

This system without any anesthetics represents the control system, and has been used as a reference for structural comparisons throughout the work. Three further systems were set up by randomly inserting Desflurane, Isoflurane and Sevoflurane respectively in the surrounding aqueous solvent at 12.5% anesthetic/lipid molar ratios, for a total of 4 simulated systems, using the *insert-molecules* tool of GROMACS 2021.4(Abraham et al., 2015). In particular, 100 anesthetic molecules replaced the water molecules and the concentration of 12.5% was chosen because it provides the best balance between having sufficiently high local anesthetic concentrations to enhance sampling in the simulation and remaining close to clinically significant concentrations.

The detailed composition of each simulated system is given in the following table (Table 4).

SYSTEM	LIPIDS	TIP3P WATER MOLECULES	Cl <sup>-</sup> IONS	Na <sup>+</sup> IONS	VA MOLECULES	TOTAL MOLECULES
CONTROL	800	126128	348	416	0	127692
DESFLURANE	800	125518	348	416	100	127182
ISOFLURANE	800	125416	348	416	100	127080
SEVOFLURANE	800	125433	348	416	100	127097

Table 4- Components of the 4 simulated systems.

## 4.2.2 Molecular Dynamics

First, all four molecular systems were subjected to whole-system energy minimization and equilibration phase employing the minimization protocol suggested by CHARMM-GUI as a starting template. Energy minimization has been performed through the Steepest Descent(Fletcher & Powell, 1963) method for 10000 steps. The Particle Mesh Ewald (PME) algorithm was employed to treat electrostatic interactions, and 1.2 nm Van der Waals and Coulomb cut-off values have been used. Periodic boundary conditions have been applied in all three dimensions x,y and z. Subsequently, the four systems were subjected to six equilibration steps, with gradually reduced position restrains (

Table 5), modeled with the standard procedures used by CHARMM-GUI. The protocol includes two NVT equilibration steps followed by four NPT steps, for a total of 1.85 ns of simulation. The first two equilibration steps are NVT simulations performed for 125 ps and a timestep of 1 fs, with higher initial position restrains in the first phase. After these, four more NPT equilibrations were performed for different times by reducing position restrains. The total time of the NPT equilibration was 1,6 ns with 2 fs timestep. During this procedure, the reference temperature was maintained at  $T=303.15$  K and the pressure at  $P=1$  bar, using the Berendsen thermostat, with coupling constant  $\tau = 1$  ps and the Berendsen barostat in semi-isotropic coupling mode with coupling constant  $\tau = 5$  ps.

Equilibration Steps	Backbone (kJ mol <sup>-1</sup> nm <sup>-2</sup> )	Residues (kJ mol <sup>-1</sup> nm <sup>-2</sup> )	Lipids (kJ mol <sup>-1</sup> nm <sup>-2</sup> )	Dihedrals (kJ mol <sup>-1</sup> nm <sup>-2</sup> )
1	4000	2000	1000	1000
2	2000	1000	400	400
3	1000	500	400	200
4	500	200	200	200
5	200	50	40	100
6	50	0	0	0

Table 5- Progressive reduction of position restrains during equilibration steps.

The last step was the production MD simulation in the NPT ensemble with a Nose-Hoover thermostat and a Parrinello-Rahman barostat for 500 ns and a timestep of 2 fs, saving the coordinates every 200 ps for the complete system, and every 4 ps for the compressed system consisting only of solute, membrane and ligand.

At the end of the simulations, the periodic boundary conditions (PBC) were removed and their trajectories were visualized with the Visual Molecular Dynamics (VMD) environment.



### 4.2.3 Results

To evaluate the effect of Desflurane, Isoflurane and Sevoflurane on the GABA<sub>A</sub> receptor, several analyses were conducted on the Molecular Dynamics trajectories of the four simulated systems, to make a direct comparison.

In order to analyze the quality of the membrane model and the effects of anesthetics on it, Geometric Area-per-Lipid (gAPL) and Bilayer Thickness ( $\delta$ ) were calculated for all systems using the MDAnalysis library (Michaud-Agrawal et al., 2011) in Python (van Rossum & Drake, 2009). Specifically, gAPL was calculated as the x-y area of the simulation box divided by half the total number of lipids (400), corresponding to the number of lipids in each membrane leaflet.

The bilayer thickness was obtained by selecting the P atoms of each leaflet and their mean z-coordinates were calculated by fitting two x-y planes. The measure of thickness is precisely the distance between these two planes, i.e. the difference between the mean z-coordinates of the P atoms in the bilayer. Desflurane, Isoflurane and Sevoflurane were found to reduce the membrane thickness and increase the geometric area per lipid, suggesting that anesthetics can insert between the lipids, slightly increasing their spacing. This would render the membrane less compact and thinner, potentially facilitating their lateral diffusion toward the receptor.

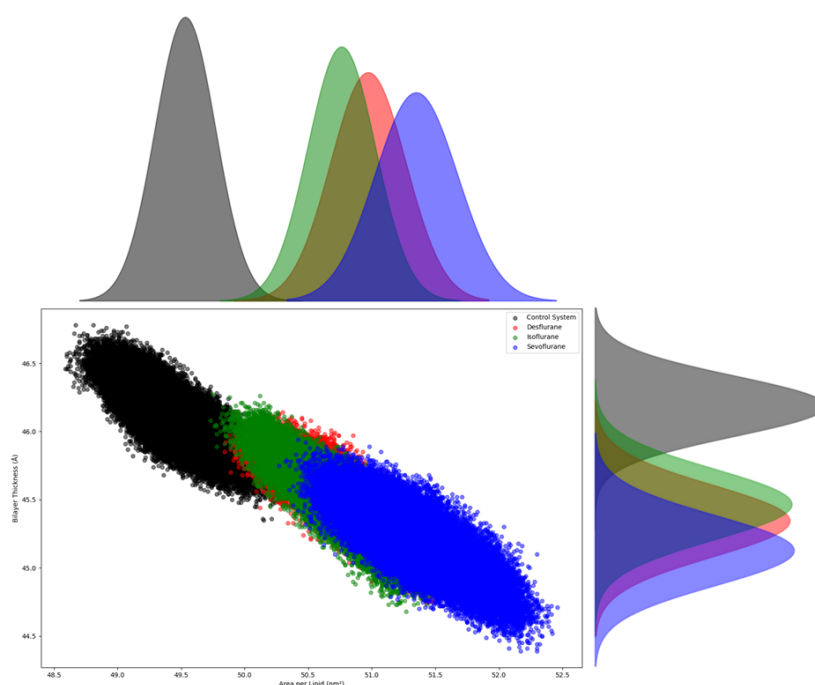


Figure 12- Relationship between membrane thickness and area per lipid in the different simulated systems. The points represent data extracted from the simulations, with the control system in black and the anesthetic-treated systems in distinct colors (Desflurane in red, Isoflurane in green, Sevoflurane in blue). The marginal distributions show the density distributions for each parameter.

Alterations in membrane properties could influence the structural and dynamic behavior of embedded proteins, for this purpose a stability analysis of the receptor was performed. The Root Mean Square Deviation (RMSD) of the protein backbone was calculated for every frame of the trajectories, showing that both the control system and the systems with anesthetics reach a stable plateau after the first 150 ns of simulation. This indicates that anesthetics don't significantly alter the overall stability of the protein. The Isoflurane system shows the highest RMSD of all systems ( $\sim 0.25$  nm), suggesting greater flexibility than the others. In contrast, the Desflurane and Sevoflurane systems show values more similar to the control ( $\sim 0.2$  nm), indicating that these anesthetics do not induce significant structural changes.

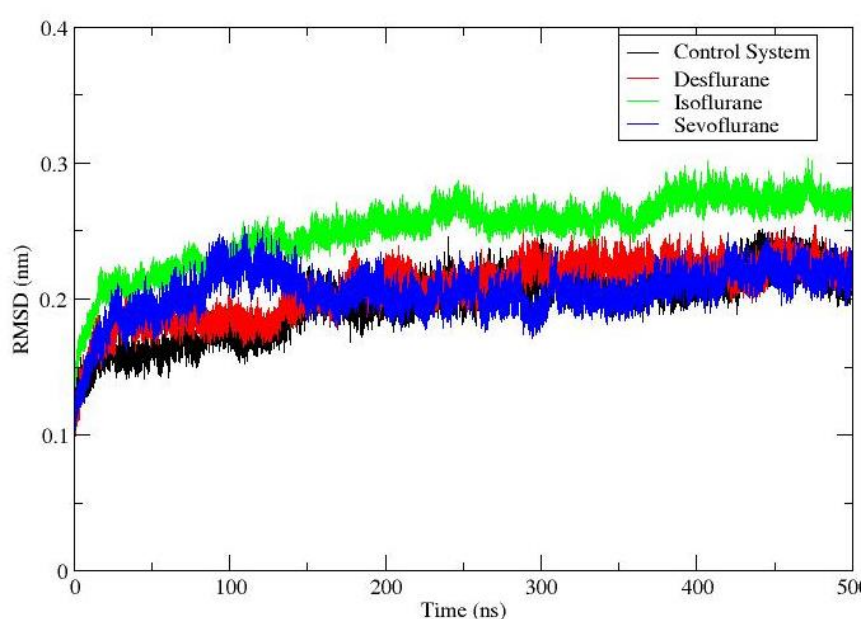


Figure 13- RMSD comparison between control system (black) and simulations with Desflurane (red), Isoflurane (green) and Sevoflurane (blue).

The Root Mean Square Fluctuation (RMSF) was calculated to analyze the fluctuations of individual residues and identify particularly mobile regions. This analysis was performed separately for each individual chain forming the pentamer, to inspect whether the ligands influence the stability and fluctuations of the side chains. RMSF data showed that some groups of residues exhibit significant differences in the presence of VAs compared to the control condition. Residues with the highest fluctuation for chains A, B, C, D and E are respectively Ser201 in the system with Desflurane, Arg187 in the system with Isoflurane, Phe200 in both the Isoflurane and Desflurane systems, His110 in the Sevoflurane system and Lys312 in the Desflurane system, and finally, Arg185 in the Isoflurane system.

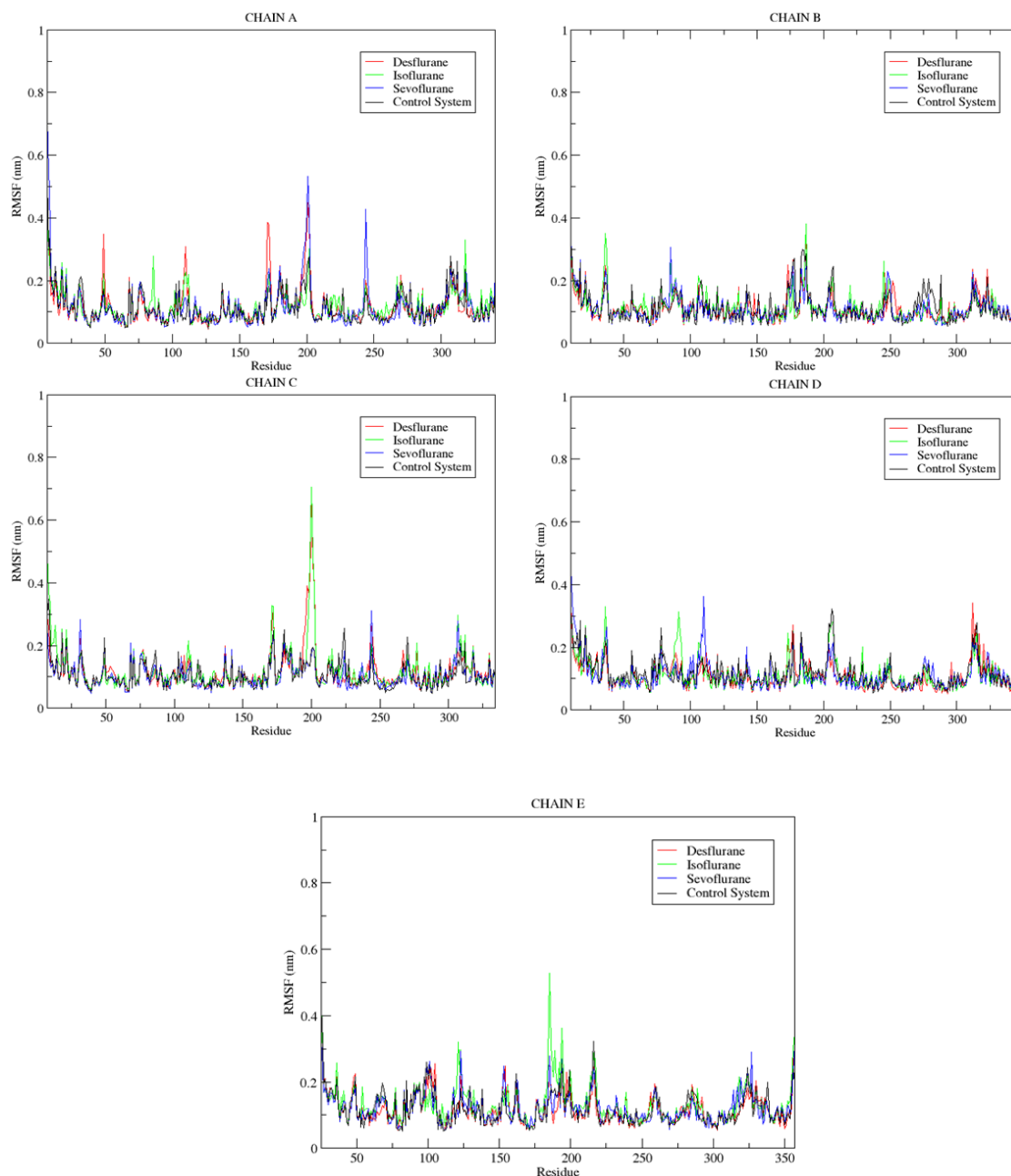


Figure 14- Root Mean Square Fluctuation (RMSF) for different protein chains (A, B, C, D, and E) in the presence of anesthetics (Desflurane in red, Isoflurane in green, Sevoflurane in blue) and in the control system (black). The RMSF values indicate the flexibility of each residue, with peaks corresponding to regions of higher mobility.

The analysis of partial density along the Z coordinate was used to determine the spatial distribution of anesthetics within the membrane. Starting from the system topology, a script generated an index file defining separate groups for the different membrane components: heads, tails, glycerol groups, cholesterol, and ligands. Subsequently, for each group, the density distribution along the Z coordinate was calculated using the *density* tool of GROMACS. The results were plotted in a single graph to

visualize the comparative distribution of the different membrane components and anesthetics (Figure 15).

The findings show that, in the systems with Isoflurane, Desflurane, and Sevoflurane, anesthetics tend to accumulate predominantly near the water-lipid interface. This suggests that their access to the receptor is not random but influenced by their initial interaction with the membrane. To further investigate this aspect, contact probability analysis was performed to determine whether anesthetics establish interactions primarily from the membrane or if direct binding from the aqueous phase also occurs.

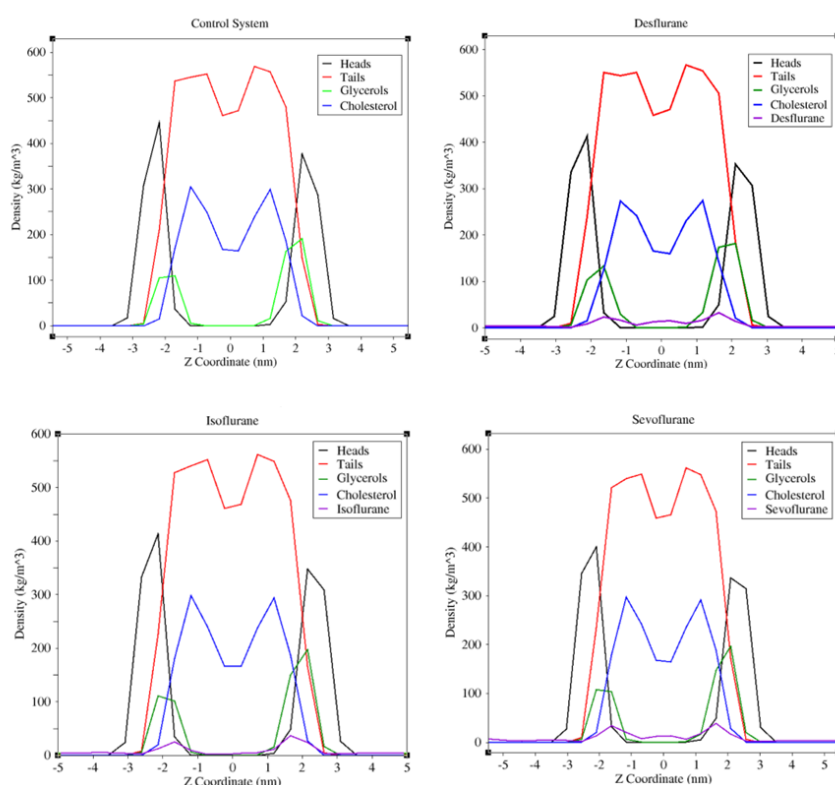


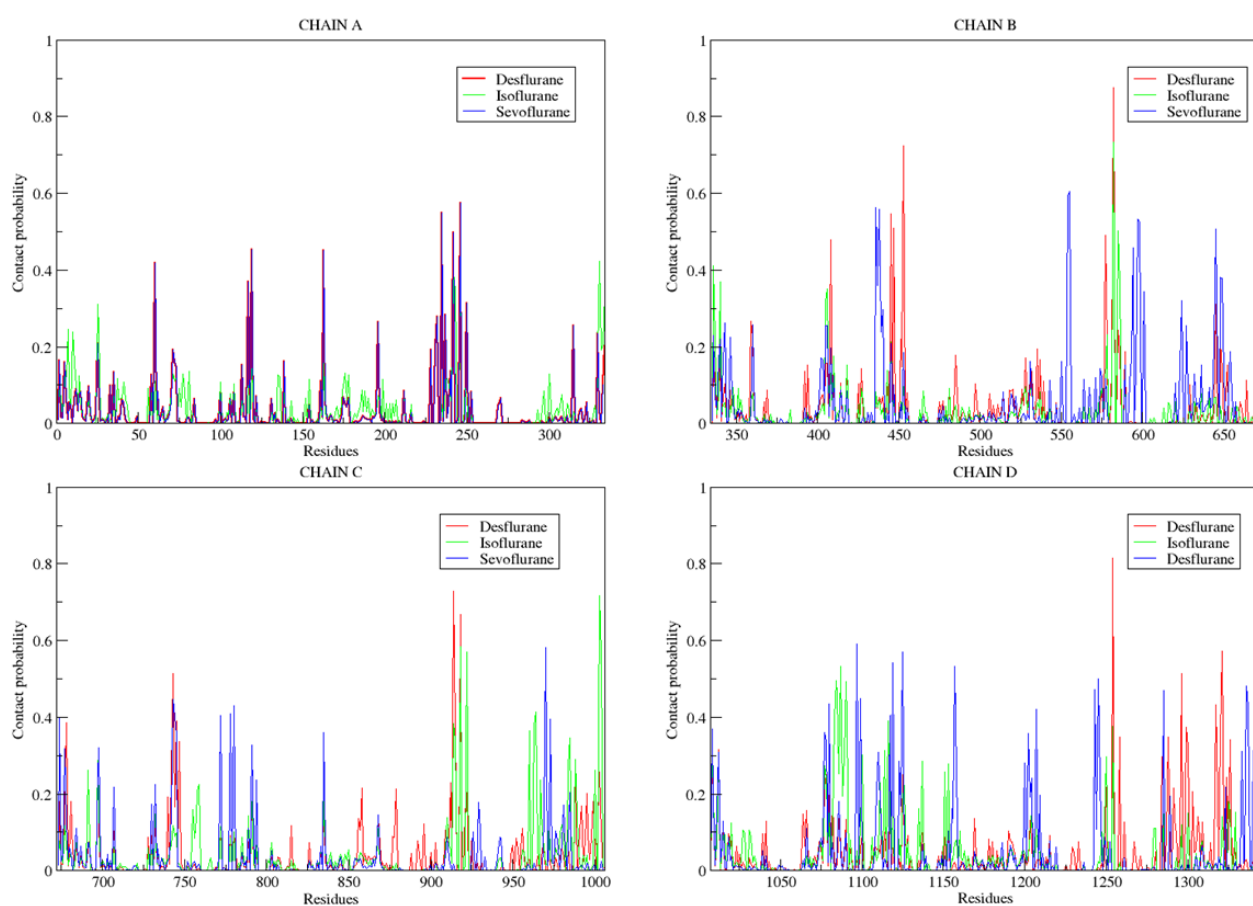
Figure 15- Density profiles along the Z-coordinate for different membrane components (heads in black, tails in red, glycerols in green, and cholesterol in blue) in the control system and in the presence of anesthetics (Desflurane, Isoflurane, and Sevoflurane)

Thanks to the solvent-like behavior of anesthetics that makes it difficult to identify static binding regions, the contact probability analysis was performed to map their interaction zones on the receptor. For each frame of the simulation, the minimum distance between each protein residue and any anesthetic molecule in the system was computed using GROMACS. Subsequently, a custom Bash script processed the contact probability for each residue by averaging the interactions detected in each frame between the residues and the ligands. An anesthetic was considered in contact with a residue when the distance between them was less than 0.28 nm. Then a comprehensive map of the contact

probability between the anesthetics and the protein residues throughout the entire simulated trajectory was obtained. However, for clarity, the individual chains of the various systems were compared.

The integration of contact probability data with density profiles along the membrane the identification of likely access routes of anaesthetics to their binding sites. The data indicate that interactions occur both in the extracellular domain and within the transmembrane region. However, contacts within the transmembrane domain, particularly inside the pore region, are more frequent, supporting the idea that anesthetics preferentially access the receptor by first partitioning into the membrane and then diffusing laterally.

By integrating these results with the analysis of local fluctuations (RMSF), it was possible to assess whether the regions of higher mobility coincide with the preferential interaction sites of anesthetics. The resulting plots show that the contact probability is not uniformly distributed along the protein sequence but is concentrated in specific regions, including the pore region, which do not coincide with the residues exhibiting the highest fluctuations. This observation suggests that the effect of anesthetics on the receptor may be predominantly allosteric rather than due to direct interaction with these highly mobile regions.



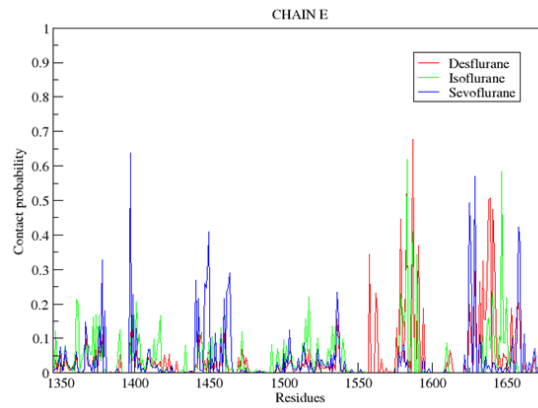


Figure 16- Probability of contact between anesthetics (Desflurane in red, Isoflurane in green, Sevoflurane in blue) and protein residues for different chains (A, B, C, D, and E). The y-axis represents the probability of a given residue being in contact with an anesthetic during the simulation. Peaks indicate residues with a high likelihood of interaction, suggesting potential binding sites or regions influenced by anesthetic presence. Notably, specific residues exhibit preferential interactions with anesthetics, which may contribute to localized structural or functional effects on the ion channel

Furthermore, the evidence that, mainly in the Desflurane and Isoflurane systems, some of the residues with the highest contact probability are predominantly located within the receptor pore, which is a critical region responsible for chloride ion permeation, suggests that anesthetics could directly influence the dynamics of ion conduction by interacting with key residues lining the pore. To illustrate this observation, a contact probability map is provided, highlighting the preferential interaction sites of anesthetics within the channel and on the receptor.

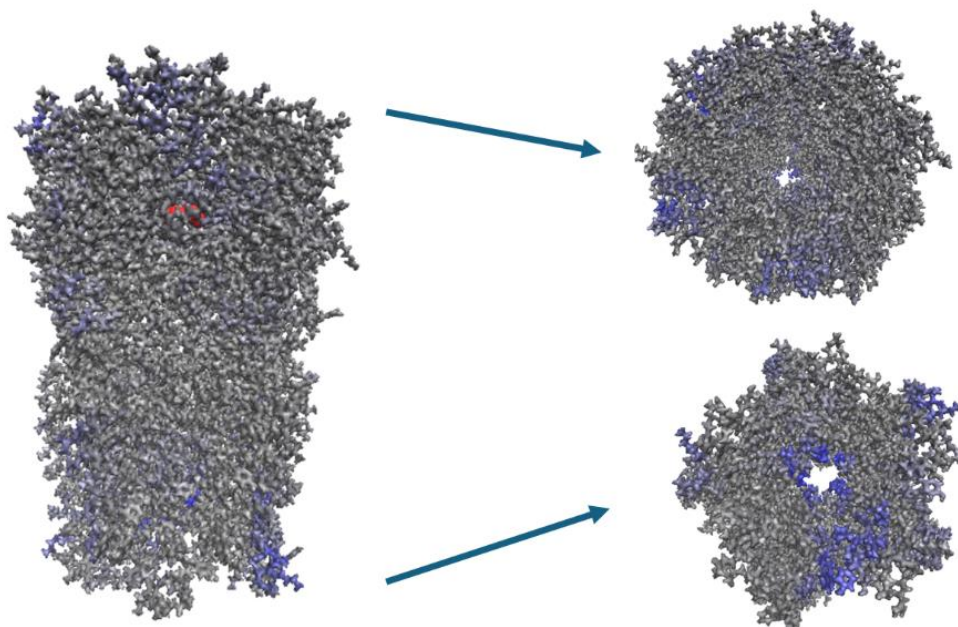


Figure 17- Contact map of the system with Desflurane, highlighting its preferential localization in the central part of the pore. The left panel shows a side view of the ion channel, with the GABA molecules (red) bound to its binding site. The right panels display top-down cross-sections, revealing regions (in blue) where Desflurane establishes frequent contacts with the protein. The preferential localization of the anesthetic in the central pore suggests potential interactions that could modulate the channel's function.

Sevoflurane, on the other hand, is positioned more randomly, however it has been observed that the Phe77 residue of the extracellular region of the receptor has a high probability of contact with it. This same residue is known to be involved in the binding of benzodiazepines, suggesting a possible direct competition between these two substances in the modulation of the GABA<sub>A</sub> receptor.

Contact analysis revealed that anesthetics interact with the GABA<sub>A</sub> not randomly, but with preferential interaction zones. These interactions occur mainly via hydrophobic interactions and van der Waals forces; however, occasional hydrogen bonds (maximum two) were also observed. To further investigate the role of hydrogen bonding in these interactions, a detailed analysis was conducted. It was observed that in the absence of anesthetic molecules, there is a slightly higher number of H-bonds within the protein (Figure 18). The anesthetics might be disrupting these H-bonds by inserting themselves between the chains, thereby facilitating their relative motions. This is particularly interesting considering that the activation of this type of receptor occurs precisely through relative displacements between adjacent chains.

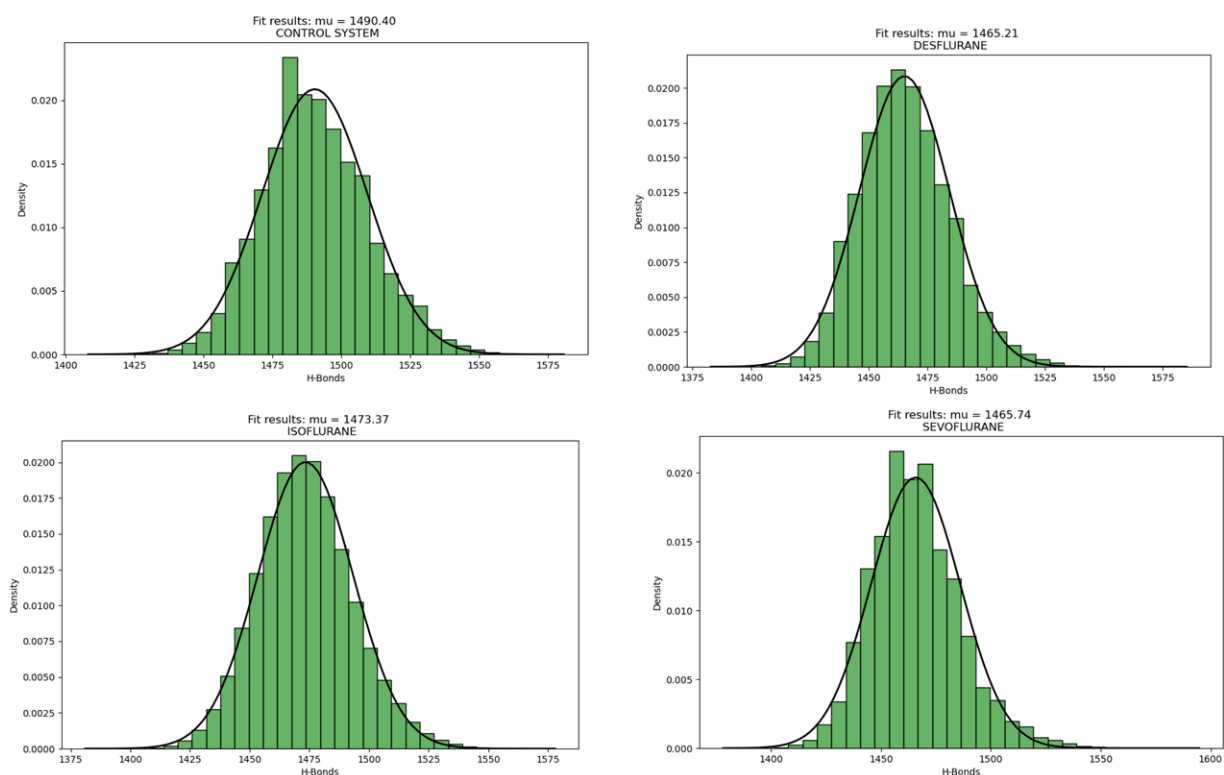
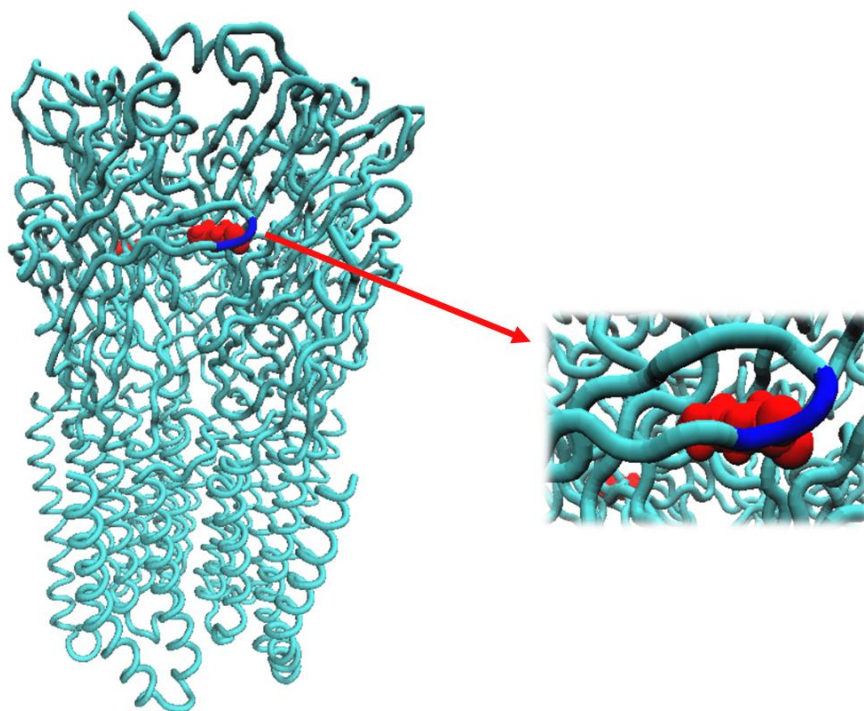


Figure 18- Distribution of the number of hydrogen bonds within the protein for the four simulated systems: Control system (top left), Desflurane system (top right), Isoflurane system (bottom left), and Sevoflurane system (bottom right). The histograms show the density distribution of hydrogen bonds, with a fitted curve highlighting the mean values ( $\mu$ ). The presence of anesthetics leads to a slight reduction in the average number of hydrogen bonds compared to the control system, suggesting a potential destabilization of intra-protein interactions.



The dynamic nature of these ligands that continuously associate and dissociate from the receptor, combined with the contact map that showed preferential zones of interaction, motivated the subsequent analysis of the conformational behavior of the receptor. To achieve this goal and to isolate the low-frequency modes that capture functionally relevant conformational dynamics, Principal Component Analysis (PCA) was applied to the backbone atoms of the protein. While the control system exhibits more stable dynamics, the presence of anesthetics induces variations in the mobility of specific regions, with effects that appear to be allosteric rather than direct. This observation is consistent with the RMSD and RMSF analyses described above, confirming that anesthetics do not dramatically alter the global stability of the receptor, but induce localized changes in the flexibility of some regions. PCA reveals the presence of hinging movements in some regions of the protein, which are absent in the control system. In particular, these movements involve residues such as Phe140 of the C chain in the Desflurane and Isoflurane systems and Ser201 of the A chain in the Sevoflurane system, which show a more pronounced shift. Interestingly, these residues are located close to the orthosteric binding site of GABA, suggesting that the presence of anesthetics can modulate the local conformational dynamics of this region. This effect strengthens the hypothesis that anesthetics influence the receptor function through allosteric mechanisms.



*Figure 19- Structural representation of the receptor highlighting the region affected by anesthetic-induced conformational changes. The left panel shows the full receptor structure, while the right panel provides a zoomed-in view of the specific region exhibiting altered flexibility (in blue). These residues, which undergo significant shifts in response to anesthetic binding, are located near the orthosteric GABA (in red) binding site.*



For each system, the Solvent Accessible Surface Area (SASA)(Ali et al., 2014) was also calculated, a crucial parameter that indicates the portion of the surface that can interact with the solvent. This value is determined by considering an idealized sphere representing a solvent molecule that rolls over the protein surface, interacting with its van der Waals surface. The results show that the control system has the lowest SASA value, indicating a more compact conformation. In the presence of anesthetics, SASA progressively increases, with Isoflurane showing the most pronounced effect. This suggests that anesthetics may promote greater exposure of the protein surface to the solvent, potentially modulating receptor dynamics and increasing flexibility induced by anesthetic binding.

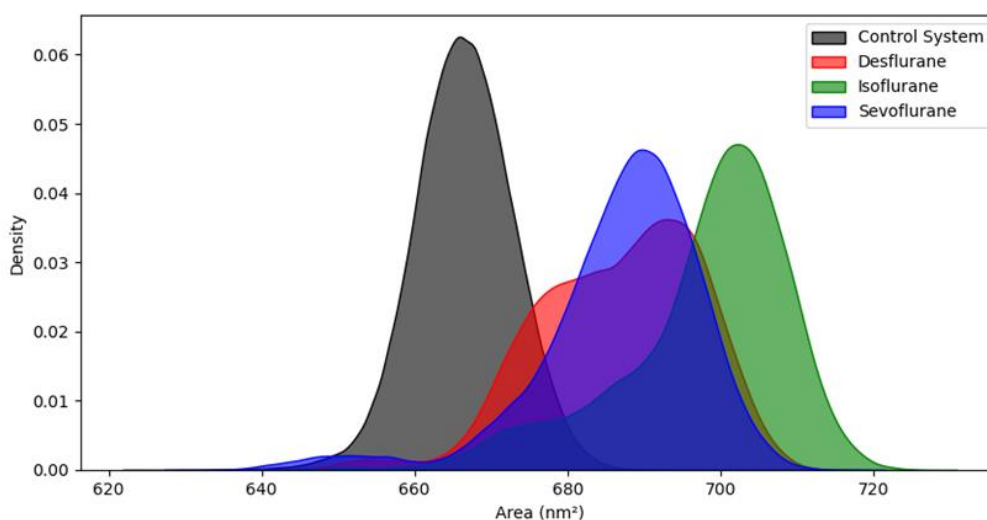


Figure 20- Distribution of the Solvent Accessible Surface Area (SASA) for the anesthetic systems (Desflurane in red, Isoflurane in blue, Sevoflurane in green) compared to the control system (black). The shift towards higher SASA values in the presence of anesthetics suggests an increase in protein exposure to the solvent.

Finally, the models were analyzed in terms of secondary structures using DSSP (Dictionary of Secondary Structure of Proteins), an algorithm designed to standardize secondary structure assignment. In this case, the individual chains of all four systems were analyzed separately, reporting the percentage of secondary structure for each residue in the chain, showing no differences in the distribution of  $\alpha$ -helices,  $\beta$ -sheets, and coils. This indicates that, although anesthetics may influence protein dynamics, they do not cause a rearrangement of the secondary structure of the GABA<sub>A</sub> receptor.

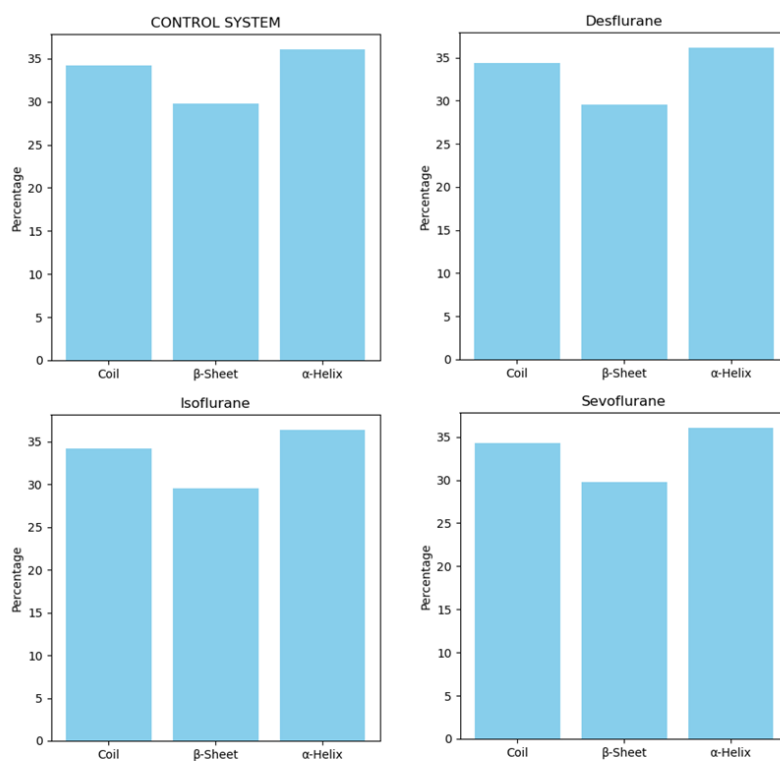


Figure 21- Percentage of coil,  $\beta$ -sheets, and  $\alpha$ -helices in the simulated systems: Control system (top left), Desflurane system (top right), Isoflurane system (bottom left), and Sevoflurane system (bottom right). The graphs show that the overall distribution of secondary structure elements remains largely unchanged across the different conditions, suggesting that the presence of anesthetics does not significantly alter the global secondary structure of the protein.

### 4.3 Discussion

Previous studies have suggested that volatile anesthetics modulate GABAergic transmission by interacting with the GABA<sub>A</sub> receptor, indicating that these molecules can act either through direct interaction with the neurotransmitter binding site or by allosterically modifying the receptor function.(Franks & Lieb, 1994)

Based on these findings, this study aimed to investigate the molecular interactions between gaseous anesthetics and the GABA<sub>A</sub> receptor using molecular dynamics simulations. Specifically, the analysis focuses on characterizing their binding behavior, spatial distribution relative to the receptor, and potential effects on its conformational dynamics.

Among the key aspects of the effect of anesthetics is their mode of access to the receptor. Partial density profiling along the Z-coordinate revealed that anesthetics are localized near the lipid-water interface and not uniformly diffused across the membrane. This is consistent with previous studies for other anesthetics (Kim et al., 2020)-(Zizzi et al., 2022), which describe the lateral diffusion of gaseous anesthetics within lipid domains, before reaching their protein target sites. Furthermore, the observed increase in area per lipid and reduction in membrane thickness in systems with anesthetic suggest that these molecules could alter the physical properties of the membrane, making it more fluid and facilitating their movement towards the receptor.

Contact probability analysis revealed that anesthetics interact predominantly with residues located within the receptor pore, which is a functional region responsible for chloride ion permeation. This finding is particularly interesting, as it suggests that anesthetics could directly influence channel gating and ion permeation dynamics. Specifically, residues with the highest contact probability are located at key positions within the transmembrane region, close to the M2 helices, which form the lining of the ion pore.

A distinctive aspect that emerges from this analysis is that volatile anesthetics occupy more central positions in the pore than intravenous anesthetics (IV), which localize between the subunits.(Kim et al., 2020) This could indicate a different mode of action, in which volatile anesthetics directly influence the ionic permeability rather than stabilizing the interactions between the protein subunits.

Root Mean Square Fluctuation (RMSF) and Principal Component Analysis (PCA) revealed a remarkable effect of anesthetics on the conformational mobility of the receptor. It was found that in

the presence of anesthetics, the residues with the highest fluctuation do not coincide with those with high contact probability, but some of them are located close to the GABA binding site. This suggests that the effect of these molecules could be allosteric rather than due to a direct interaction with the most mobile residues. PCA analysis highlighted that a lateral solvent-exposed loop formed by residues Phe200 in Desflurane and Isoflurane systems and Ser201 in the Sevoflurane system, show significant shifts compared to the control system.

The C-loop, which includes the above-mentioned residues Phe200 and Ser201, is a flexible structure located in the extracellular domain of the GABA<sub>A</sub> receptor, close to the GABA binding site. Functionally, this loop is involved in the recognition and capture of the neurotransmitter, contributing to the stabilization of the ligand-receptor complex and to the signal transduction leading to the opening of the channel.(P. S. Miller & Aricescu, 2014) The increased fluctuation of this loop in the presence of anesthetics compared to the control system, could facilitate the binding of GABA or influence the conformational transition of the receptor to the active state, suggesting a mechanism of potentiation of the inhibitory action of the receptor.

This hypothesis is further validated by hydrogen bond analysis. In systems simulated with anesthetics we observed a slight reduction in the number of hydrogen bonds between the protein and itself, suggesting that their presence may promote greater relative mobility of the subunits. Since the activation of this type of receptor is known to involve movements between adjacent receptor chains, the correlation of this finding with the greater fluctuations observed with anesthetics suggests that these conformational transitions make the receptor more prone to activation in response to GABA binding. This effect can be responsible for enhancement of GABAergic inhibition, prolonging channel opening time and increasing the effect of the neurotransmitter.

These results suggest that the action of volatile anesthetics on the GABA<sub>A</sub> receptor is not through stabilization of the open state, as seen with benzodiazepines and IV anesthetics, but through a change of the energetic landscape of the channel's conformational dynamics, making the closed state less stable.(Kim et al., 2020) Their position in the ion pore and interaction with the M2 helices may disrupt the forces that stabilize the channel in the closed state. In contrast, increased mobility of the C-loop, highlighted by PCA analysis, is indicative of increased flexibility within a functionally relevant region for GABA recognition and signal transduction.

Generally, all these effects might predispose the receptor to being more readily activated, lowering the threshold for GABA-induced channel opening. This is the basis of the enhancement of GABAergic action by volatile anesthetics and subsequent amplification of neuronal inhibition.

## 4.4 Conclusion

In this study the molecular interaction between the volatile anesthetics Desflurane, Isoflurane and Sevoflurane and the GABA<sub>A</sub> ion channel receptor in complex with its natural ligand GABA was investigated. The GABA<sub>A</sub> subtype  $\alpha 1\beta 2\gamma 2$  in complex with GABA and inserted in a phospholipid bilayer is simulated using the Molecular Dynamics workflow, with a given concentration of anesthetics. This approach confirmed that Isoflurane, Sevoflurane and Desflurane directly interact with the receptor, furthermore suggesting a mechanism of action based on allosteric modulation, whereby anesthetics bind in areas other than the GABA binding site. The analysis of the spatial distribution of the anesthetics showed that these compounds do not spread uniformly in the membrane, but tend to localize in specific region, from which they access on their interaction sites on the protein. Furthermore, it was possible to identify the main contact areas between anesthetics and the receptor, highlighting potential modulation sites. Interactions in the internal part of the transmembrane channel domain can generate conformational protein changes, which could influence directly the process of opening/closing of the ionic pore. Overall, these results are consistent with the model in which volatile anesthetics act through a series of direct interaction with the receptor and allosteric modification of its structural dynamics, favoring the predisposition of the channel toward activation. This study contributes to the understanding of the mechanism of action of anesthetics and lays the foundation for future research to further define their role in the modulation of GABAergic transmission. More detailed investigation of these actions could have important implications in the development of new anesthetics with greater selectivity and reduced side effects.

## 5. References

A Broyden—Fletcher—Goldfarb—Shanno optimization procedure for molecular geometries *ScienceDirect*. (n.d.). Retrieved September 9, 2024, from <https://www.sciencedirect.com/science/article/abs/pii/0009261485805741>

Abraham, M. J., Murtola, T., Schulz, R., Páll, S., Smith, J. C., Hess, B., & Lindahl, E. (2015). GROMACS: High performance molecular simulations through multi-level parallelism from laptops to supercomputers. *SoftwareX*, 1–2, 19–25. <https://doi.org/10.1016/j.softx.2015.06.001>

Admin. (2024, November 26). Recettore glicinergico (o della glicina) A. *Medicinapertutti.it*. <https://www.medicinapertutti.it/argomento/recettore-glicinergico-o-della-glicina-a/>

Ali, S. A., Hassan, M. I., Islam, A., & Ahmad, F. (2014). A review of methods available to estimate solvent-accessible surface areas of soluble proteins in the folded and unfolded states. *Current Protein & Peptide Science*, 15(5), 456–476. <https://doi.org/10.2174/1389203715666140327114232>

Antkowiak, B. (2001). How do general anaesthetics work? *Die Naturwissenschaften*, 88, 201–213. <https://doi.org/10.1007/s001140100230>

Baldassarre, D., Scarpati, G., & Piazza, O. (2020). *Mechanisms of Action of Inhaled Volatile General Anesthetics: Unconsciousness at the Molecular Level* (pp. 109–123). [https://doi.org/10.1007/978-1-4939-9891-3\\_6](https://doi.org/10.1007/978-1-4939-9891-3_6)

Bauer, P., Hess, B., & Lindahl, E. (2022). *GROMACS 2022 Manual*. <https://doi.org/10.5281/ZENODO.6103568>

Berman, H. M. (2000). The Protein Data Bank. *Nucleic Acids Research*, 28(1), 235–242. <https://doi.org/10.1093/nar/28.1.235>

Bernard, C. (1870). On the Combined Action of Morphia and Chloroform. *Buffalo Medical and Surgical Journal*, 10(3), 108–109.

Bertaccini, E. J. (2010). The Molecular Mechanisms of Anesthetic Action: Updates and Cutting Edge Developments from the Field of Molecular Modeling. *Pharmaceuticals*, 3(7), Article 7. <https://doi.org/10.3390/ph3072178>

Campagna, J. A., & Forman, S. A. (2003). 030522 Mechanisms of Actions of Inhaled Anesthetics. *Drug Therapy*.

Campagna, J. A., Miller, K. W., & Forman, S. A. (2003). Mechanisms of Actions of Inhaled Anesthetics. *New England Journal of Medicine*, 348(21), 2110–2124. <https://doi.org/10.1056/NEJMra021261>

Cecchini, M., Corringer, P.-J., & Changeux, J.-P. (n.d.). *The nicotinic acetylcholine receptor and its pentameric homologues: Towards an allosteric mechanism of signal transduction at the atomic level*.

*CHARMM-GUI Membrane Builder toward realistic biological membrane simulations—Wu—2014—Journal of Computational Chemistry—Wiley Online Library*. (n.d.). Retrieved October 22, 2024, from <https://onlinelibrary.wiley.com/doi/abs/10.1002/jcc.23702>

Chau, P.-L. (2010). New insights into the molecular mechanisms of general anaesthetics. *British Journal of Pharmacology*, 161(2), 288–307. <https://doi.org/10.1111/j.1476-5381.2010.00891.x>

*Do general anaesthetics act by competitive binding to specific receptors?* | *Nature*. (n.d.). Retrieved October 11, 2024, from <https://www.nature.com/articles/310599a0>

E, O. C. (1991). Studies of narcosis and a contribution to general pharmacology. *Studies of Narcosis*. <https://cir.nii.ac.jp/crid/1570854175373998208>

faadmin. (n.d.). *CGENFF By SilcsBio*. CGENFF. Retrieved October 22, 2024, from <https://cgenff.com/>

Fletcher, R., & Powell, M. J. D. (1963). A Rapidly Convergent Descent Method for Minimization. *The Computer Journal*, 6(2), 163–168. <https://doi.org/10.1093/comjnl/6.2.163>

Flood, P., & Role, L. W. (1998). Neuronal nicotinic acetylcholine receptor modulation by general anesthetics. *Toxicology Letters*, 100–101, 149–153. [https://doi.org/10.1016/S0378-4274\(98\)00179-9](https://doi.org/10.1016/S0378-4274(98)00179-9)

Franks, N. P., & Lieb, W. R. (1994). Molecular and cellular mechanisms of general anaesthesia. *Nature*, 367(6464), 607–614. <https://doi.org/10.1038/367607a0>

Frazer, A., & Hensler, J. G. (1999). Serotonin Receptors. In *Basic Neurochemistry: Molecular, Cellular and Medical Aspects*. 6th edition. Lippincott-Raven. <https://www.ncbi.nlm.nih.gov/books/NBK28234/>

Ghit, A., Assal, D., Al-Shami, A. S., & Hussein, D. E. E. (2021). GABAA receptors: Structure, function, pharmacology, and related disorders. *Journal of Genetic Engineering and Biotechnology*, 19(1), 123. <https://doi.org/10.1186/s43141-021-00224-0>

Hassaine, G., Deluz, C., Grasso, L., Wyss, R., Tol, M. B., Hovius, R., Graff, A., Stahlberg, H., Tomizaki, T., Desmyter, A., Moreau, C., Li, X.-D., Poitevin, F., Vogel, H., & Nury, H. (2014). X-ray structure of the mouse serotonin 5-HT<sub>3</sub> receptor. *Nature*, 512(7514), Article 7514. <https://doi.org/10.1038/nature13552>

Herold, K., & Hemmings, H. (2012). Sodium Channels as Targets for Volatile Anesthetics. *Frontiers in Pharmacology*, 3. <https://www.frontiersin.org/articles/10.3389/fphar.2012.00050>

Hollingsworth, S. A., & Dror, R. O. (2018). Molecular Dynamics Simulation for All. *Neuron*, 99(6), 1129–1143. <https://doi.org/10.1016/j.neuron.2018.08.011>



Howard, R. J., Trudell, J. R., & Harris, R. A. (2014). Seeking Structural Specificity: Direct Modulation of Pentameric Ligand-Gated Ion Channels by Alcohols and General Anesthetics. *Pharmacological Reviews*, 66(2), 396–412. <https://doi.org/10.1124/pr.113.007468>

*Ion Channel | Learn Science at Scitable*. (n.d.). Retrieved October 5, 2024, from <https://www.nature.com/scitable/topicpage/ion-channel-14047658/>

Jo, S., Kim, T., Iyer, V. G., & Im, W. (2008). CHARMM-GUI: A web-based graphical user interface for CHARMM. *Journal of Computational Chemistry*, 29(11), 1859–1865. <https://doi.org/10.1002/jcc.20945>

Kim, J. J., Gharpure, A., Teng, J., Zhuang, Y., Howard, R. J., Zhu, S., Noviello, C. M., Walsh, R. M., Lindahl, E., & Hibbs, R. E. (2020). Shared structural mechanisms of general anaesthetics and benzodiazepines. *Nature*, 585(7824), 303–308. <https://doi.org/10.1038/s41586-020-2654-5>

Leach, A. R. (2001). *Molecular Modelling: Principles and Applications*. Pearson Education.

McCarthy, J. F. (1989). Block-conjugate-gradient method. *Physical Review D*, 40(6), 2149–2152. <https://doi.org/10.1103/PhysRevD.40.2149>

McCormick, D. A. (1989). GABA as an inhibitory neurotransmitter in human cerebral cortex. *Journal of Neurophysiology*, 62(5), 1018–1027. <https://doi.org/10.1152/jn.1989.62.5.1018>

Michaud-Agrawal, N., Denning, E. J., Woolf, T. B., & Beckstein, O. (2011). MDAAnalysis: A toolkit for the analysis of molecular dynamics simulations. *Journal of Computational Chemistry*, 32(10), 2319–2327. <https://doi.org/10.1002/jcc.21787>

Mihic, S. J., & Harris, R. A. (1997). GABA and the GABAA Receptor. *Alcohol Health and Research World*, 21(2), 127–131.

Miller, P. S., & Aricescu, A. R. (2014). Crystal structure of a human GABAA receptor. *Nature*, 512(7514), 270–275. <https://doi.org/10.1038/nature13293>

Miller, R. D., Eriksson, L. I., Fleisher, L. A., Wiener-Kronish, J. P., Cohen, N. H., & Young, W. L. (2014). *Miller's Anesthesia E-Book*. Elsevier Health Sciences.

*Molecular Operating Environment (MOE) | MOEsaic | PSILO*. (n.d.). Retrieved October 22, 2024, from <https://www.chemcomp.com/en/Products.htm>

Notman, R., & Anwar, J. (2015). *ModellingOfMembranesReview Anwar ADDR 2012* [Dataset].

Olsen, R. W., & Sieghart, W. (2009). GABAA receptors: Subtypes provide diversity of function and pharmacology. *Neuropharmacology*, 56(1), 141–148. <https://doi.org/10.1016/j.neuropharm.2008.07.045>

Pauling, L., & Wilson, E. B. (2012). *Introduction to Quantum Mechanics with Applications to Chemistry*. Courier Corporation.

Pohorille, A., Wilson, M. A., New, M. H., & Chipot, C. (1998). Concentrations of anesthetics across the water–membrane interface; the Meyer–Overton hypothesis revisited. *Toxicology Letters*, 100–101, 421–430. [https://doi.org/10.1016/S0378-4274\(98\)00216-1](https://doi.org/10.1016/S0378-4274(98)00216-1)

Russell, D., & Kenny, G. N. C. (1992). 5-HT 3 Antagonists in Postoperative Nausea and Vomiting. *British Journal of Anaesthesia*, 69, 63S–68S. [https://doi.org/10.1093/bja/69.supplement\\_1.63S](https://doi.org/10.1093/bja/69.supplement_1.63S)

Schlick, T. (2010). *Molecular Modeling and Simulation: An Interdisciplinary Guide: An Interdisciplinary Guide* (Vol. 21). Springer New York. <https://doi.org/10.1007/978-1-4419-6351-2>

*Sites of alcohol and volatile anaesthetic action on GABAA and glycine receptors* | *Nature*. (n.d.). Retrieved February 23, 2025, from <https://www.nature.com/articles/38738>

Sittel, F., Jain, A., & Stock, G. (2014). Principal component analysis of molecular dynamics: On the use of Cartesian vs. internal coordinates. *The Journal of Chemical Physics*, *141*, 014111. <https://doi.org/10.1063/1.4885338>

Skeel, R. D. (2009). What Makes Molecular Dynamics Work? *SIAM Journal on Scientific Computing*, *31*(2), 1363–1378. <https://doi.org/10.1137/070683660>

Tassonyi, E., Charpantier, E., Muller, D., Dumont, L., & Bertrand, D. (2002). The role of nicotinic acetylcholine receptors in the mechanisms of anesthesia. *Brain Research Bulletin*, *57*(2), 133–150. [https://doi.org/10.1016/S0361-9230\(01\)00740-7](https://doi.org/10.1016/S0361-9230(01)00740-7)

*The Newton-Raphson method: International Journal of Mathematical Education in Science and Technology: Vol 26 , No 2—Get Access*. (n.d.). Retrieved September 9, 2024, from <https://www.tandfonline.com/doi/pdf/10.1080/0020739950260202>

Tufféry, S. (2011). *Data Mining and Statistics for Decision Making*. John Wiley & Sons.

Van Der Spoel, D., Lindahl, E., Hess, B., Groenhof, G., Mark, A. E., & Berendsen, H. J. C. (2005). GROMACS: Fast, flexible, and free. *Journal of Computational Chemistry*, *26*(16), 1701–1718. <https://doi.org/10.1002/jcc.20291>

van Rossum, G., & Drake, F. L. (2009). *Introduction to PYTHON 2.6*. CreateSpace.

Vanommeslaeghe, K., Hatcher, E., Acharya, C., Kundu, S., Zhong, S., Shim, J., Darian, E., Guvench, O., Lopes, P., Vorobyov, I., & Mackerell Jr., A. D. (2010). CHARMM general force field: A force field for drug-like molecules compatible with the CHARMM all-atom additive biological force fields. *Journal of Computational Chemistry*, *31*(4), 671–690. <https://doi.org/10.1002/jcc.21367>

Vanommeslaeghe, K., Raman, E. P., & MacKerell, A. D. (2012). Automation of the CHARMM General Force Field (CGenFF) II: Assignment of bonded parameters and partial atomic charges. *Journal of Chemical Information and Modeling*, 52(12), 3155–3168. <https://doi.org/10.1021/ci3003649>

Wang, C., & Slikker, W. J. (2008). Strategies and Experimental Models for Evaluating Anesthetics: Effects on the Developing Nervous System. *Anesthesia & Analgesia*, 106(6), 1643. <https://doi.org/10.1213/ane.ob013e3181732c01>

Wang, J., Wolf, R. M., Caldwell, J. W., Kollman, P. A., & Case, D. A. (2004). Development and testing of a general amber force field. *Journal of Computational Chemistry*, 25(9), 1157–1174. <https://doi.org/10.1002/jcc.20035>

*WHO Model Lists of Essential Medicines*. (n.d.). Retrieved October 9, 2024, from <https://www.who.int/groups/expert-committee-on-selection-and-use-of-essential-medicines/essential-medicines-lists>

Zeiler, G. E., & Pang, D. S. J. (2024). *Fundamental Principles of Veterinary Anesthesia*. John Wiley & Sons.

Zizzi, E. A., Cavaglia, M., Tuszynski, J. A., & Deriu, M. A. (2022). Alteration of lipid bilayer mechanics by volatile anesthetics: Insights from  $\mu$ s-long molecular dynamics simulations. *iScience*, 25(3), 103946. <https://doi.org/10.1016/j.isci.2022.103946>